INSTITUTO
UNIVERSITÁRIO
DE LISBOA

Option Valuation with the Heston Model

Yannik Ehlert

Master in Finance

Supervisor:
PhD José Carlos Gonçalves Dias,
Associate Professor (with aggregation),
Iscte-Iul

July, 2022

BUSINESS
SCHOOL

Department of Finance

Option Valuation with the Heston Model

Yannik Ehlert

Master in Finance

PhD José Carlos Gonçalves Dias,
Associate Professor (with aggregation),
Iscte-Iul

July, 2022

Resumo

Esta tese está dividida em duas partes. A primeira parte explica os fundamentos teóricos da avaliação de opções e explica a derivação do modelo de Heston. O modelo é derivado, examinado e otimizado. Para avaliar as opções americanas também no modelo de Heston, o Método das Diferenças Finitas é aplicado no modelo de Heston. Para comparação, são apresentados o modelo Black-Scholes-Merton e o modelo de Cox-Ross-Rubinstein. A segunda parte trata de tópicos mais práticos: uma análise de parâmetros, a calibração do modelo usando dados reais de mercado e o cálculo real de preços de opções europeias e americanas com o modelo de Heston e os modelos alternativos mencionados. Para a aplicação do modelo e a derivação de todo o conteúdo gráfico, é utilizado o programa MATLAB. O foco geral está na determinação da qualidade do modelo, que será examinada comparando os valores de Heston com os dados reais do mercado e os valores dos modelos que assumem um movimento Browniano geométrico. Os resultados são avaliados criticamente em termos de precisão e esforço computacional. Por fim, vantagens e desvantagens do modelo de Heston serão discutidas.

Código de classificação: G13

Palavras chave: Opções Americanas, Modelo de Heston, Volatilidade

Abstract

This thesis is divided into two parts. The first part explains the theoretical background of option valuation and guides through the actual derivation of the Heston Model. The model is explained, examined and optimized. To value American options in the Heston model as well, the Finite Difference Method is applied in the Heston Model. For a comparison, the Black-Scholes-Merton Model and the Cox-Ross-Rubinstein Model are introduced. The second part deals with more practical topics: a parameter analysis, the calibration of the model using real market data and the actual calculation of European and American option prices with the Heston Model and mentioned peer models. For the application of the model and the derivation of all graphical content, the MATLAB program is used. The general focus lies in the determination of the quality of the model, which be examined by comparing the Heston values to the real market data and the peer model values. The results are critically evaluated in terms of accuracy and effort. Finally, advantages and disadvantages of the Heston Model will be discussed in extension.

Classification code: G13

Keywords: American Options, Heston Model, Volatility

Table of Contents

1. Introduction 1

2. Basic concepts 3

2.1. Stochastic Process 3

2.2. Wiener Process 3

2.3. Itô's Lemma 4

2.4. Volatility Smile 5

3. Valuation Methods 7

3.1. Black-Scholes-Merton Model 7

3.2. Cox-Ross-Rubinstein Method 8

4. Heston stochastic volatility Model 11

4.1. The Heston Model 11
4.1.1. Stochastic Process of the Heston Model 11
4.1.2. Risk neutral adjustments 12
4.1.3. Derivation of the Heston PDE 13
4.1.4. PDE for P1 and P2 17
4.1.5. Characteristic function 20
4.1.6. Riccati Equation 22

4.2. Problems and extensions of the Heston Model 25
4.2.1. Problems with the integrant 25
4.2.2. The Little Heston Trap 27
4.2.3. Consolidation of the integrals and Characteristic Functions 30

4.3. American Options in the Heston Model 30

5. Parameter analysis 33

5.1. Effect of the Correlation Parameter 33

5.2. Effect of the Volatility of the Variance Parameter 34

5.3. Comparison with the Black Scholes-Merton Model 34

6. Numerical analysis 37

6.1. General conditions and CPU 37

6.2. Data 37

6.3. Calibration of the model 38

6.4. Results for European call options 40

6.5. Results for American put options 45

7. Discussion 47

8. Conclusion 49

Table of Figures

Figure 2.1: Wiener Process, own representation 4
Figure 2.2: Volatility Smile, own representation 6
Figure 4.1: Discontinuities of the integrand, own representation 26
Figure 4.2: Oscillation of the integrand, own representation 27
Figure 4.3: The little Heston Trap, own representation 28
Figure 4.4: Integrand with the Albrecher et al. (2007) formulation, own representation 29
Figure 4.5: Oscillation with the Albrecher at al. (2007) formulation, own representation 29
Figure 5.1: Relationship between skewness and correlation, own representation 33
Figure 5.2: Relationship between kurtosis and volatility of the variance, own representation 34
Figure 5.3: Comparison with BSM for different correlations, own representation 35
Figure 5.4: Comparison with BSM for different volatilities of the variance, own representation 35

List of Tables

Table 6.1: Option values and implied volatilities for the S&P500 and Apple stock 38
Table 6.2: Calibrated parameters for the S&P500 options, whole sample 40
Table 6.3: Calibrated parameters for the Apple options 40
Table 6.4: Option prices for the S&P500 from the market and with the BSM Method 41
Table 6.5: Option prices for the S&P 500 with the Heston Model and its errors, whole sample 42
Table 6.6: CHJ option prices minus the BSM option prices 43
Table 6.7: Calibrated parameters for the S&P500 options, split sample 44
Table 6.8: Option prices for the S&P 500 with the Heston Model and its errors, split sample 44
Table 6.9: Calibrated parameters for the S&P500 options, FDE adjusted 45
Table 6.10: Option prices for the S&P 500 with the Heston Model (FDE) and its errors 45
Table 6.11: Option prices for the Apple stock from the market and with the CRR Method 46
Table 6.12: Option prices for Apple with the Heston Model (FDE adaption) and its errors 46

Glossary of acronyms

ATM	At-the-money
BSM	Black-Scholes-Merton
CHJ	Christoffersen et al.
CIR	Cox-Ingersoll-Ross
CRR	Cox, Ross und Rubinstein
CEV	Constant elasticity of variance
FDE	Explicit Finite Difference Method
GBM	Geometric Brownian Motion
ITM	In-the-money
IVMSE	Implied Volatility Mean Square Error
MSE	Mean Error Sum of Squares
ODE	second-order ordinary differential equation
OTM	Out-of-the-money
RMAE	Relative Mean Absolute Error
RMSE	Relative Mean Squared Error
PDE	Partial differential equation
SDE	Stochastic differential equation

Glossary of symbols

$\mathcal{A}$	generator of the Heston model
a	constant (drift)
b	constant (noise)
C	call option price
C_{tk}	call option price at time t with strike k
C_{tk}^{Θ}	call option price of a model at time t with strike k and Θ parameters
C_j	coefficient of the Heston formula of type j
D_j	coefficient of the Heston formula of type j
d	factor by which the share value decreases
dz	standard one-dimensional Brownian motion
f	function
h_t	Ornstein-Uhlenbeck Process of the volatility
IV_{tk}	implied volatility at time t with strike k
IV_{tk}^{Θ}	implied volatility of a model at time t with strike k and Θ parameters
i	imaginary unit
K	strike price
K_1	constant
κ	mean reversion speed
N	number of observations
P	put option price
$\mathbb{P}$	physical measure
$P_1 \; and \; P_2$	probability of the call option expiring ITM
p	risk-neutral probability
φ	unit of a variable
$\mathbb{Q}$	risk-neutral measure
q	dividend rate
Re	real part of the integrand
r	risk-free interest rate
S_0	initial spot price
S_t	spot price at time t

T	end of maturity
t	points in time
τ	time to maturity
U	an option of a portfolio
u	factor by which the share value increases
V	an option of a portfolio
v_0	initial variance
w_{tk}	weight of an option at time t with strike k
ω_t	volatility process at time *t* (Zhu)
Z	standard normal variable
z	Wiener Process
Π	portfolio
π	phi
ϕ	cumulative distribution function of the standard normal distribution
Δ	unit of a variable
μ	drift
σ^2	variance (BSM)
σ	volatility (BSM)
σ	volatility of the variance (Heston)
θ	long term variance
Θ	the Heston parameters
λ	volatility risk premium

1. Introduction

The financial markets play an extremely important role in the world economy. Value in form of cash, equity, debt and derivatives is floating around the globe, changing its holder frequently. The development of computational power and progress in automation made this globalization possible. Still, the underlying assumption did not change over the decades: Products are priced with its fair value. Without a doubt, pricing derivatives is the most challenging part. One kind of derivative is the financial option, whose value depends on the value of an underlying security. Samuelson (1973) already claimed decades ago that it is difficult to price financial options with its fair price.

The first ones to present an explicit solution for option values were Black and Scholes (1973) and Merton (1973). Their well-known formula works under certain conditions for European options and is often used until today. Moreover, it builds the basis for further, more complex option valuation models. The model was state-of-the-art until 1987, when the stock market crashed. At that time, it became apparent, that the model had major shortcomings. The model did not stand a real market application.

It was Heston (1993) who showed that the problem of the Black-Scholes-Merton Model lied in the assumption of constant volatility.[1] The calculated prices did not reflect the skewness and the smile of the volatility surface, and therefore the prices were inaccurate. The model needed an upgrade. The most widely idea was to replace the constant volatility with a stochastic volatility process to better reflect real life behavior of option prices. Heston (1993) introduced such a model in his publication which until today is one of the most famous ones. What makes is so famous is the fact that the method is able to deliver a closed form solution for European options, whereas many other methods need to use numerical methods to present a solution (Ruoah, 2013).

The idea is to fully understand and explain the model, test it in a comparison with real market data and other option valuation methods, e.g. the Black-Scholes-Merton Model, and finally discuss the pros and cons of it. Therefore, I start with the very basics of option valuation, the Brownian motion and the Wiener Process. I briefly introduce the Black-Scholes-Merton Model and go then deeper into the stochastic processes needed for the Heston Model. After the full derivation of the model and its extensions, first tests are done in a parameter analysis to understand the behavior of the model. The following calibration of the model and calculation of option prices represents the core of this thesis. The results are compared with other methods and real market data and are finally evaluated in an extensive discussion.

[1] The constant elasticity of variance (CEV), which was already introduced in 1975, shows an inverse relationship between the stock prices and volatilities, that is not reflected in the BSM Model (Cox, 1996).

2. Basic concepts

2.1. Stochastic Process

Due to the way option contracts are structured, their value depends on the value of the underlying, e.g. a share or an index. The values of these primary assets are linked to a random walk, meaning they can be seen as a variable that changes over time. Therefore, its value can be expressed in the form of probabilities, so that the development follows a stochastic process (Paul & Baschnagel, 2013). Stochastic processes are the bottom line for option valuation, since a time-varying variable with an uncertain development, like the underlying of the option, can best expressed with these processes. This is essential to completely understand option pricing (Hull, 2018).

2.2. Wiener Process

Since future developments naturally depend only on the current and not on past prices, the underlying process can be described with help of a Markov Process. This is a process in which the future value only depends on the present, the past is neglectable (Darling & Siegert, 1953). A special form of this process is the Wiener Process. It assumes a statistical distribution with an expected value of zero and a variance of one. The process is also known as Brownian motion or Wiener Process (Hull, 2018). Before we can use this process to replicate the movement of financial products, we need to modify some characteristics which are problematic for us. Firstly, it assumes a mean change of zero, which is not the general case for stocks. Secondly, the process assumes the same variance for all stocks, which obviously does not hold in practice as well. Lastly, the Brownian motion can deliver negative stock values, which cannot appear in practice. To solve the issues one and two, we can complement the Brownian motion with a drift rate to receive the generalized Wiener Process. The drift rate describes the median change of the value per time. Expressed in mathematical terms, we now have

$$\boldsymbol{dx = a\,dt + b\,dz}, \tag{2.1}$$

where a represents the drift rate for the chance over time dt and b adds a variability factor for the volatility dz. Both a and b are constants here. To conclude this, we can see the graph representing the different components we just used.

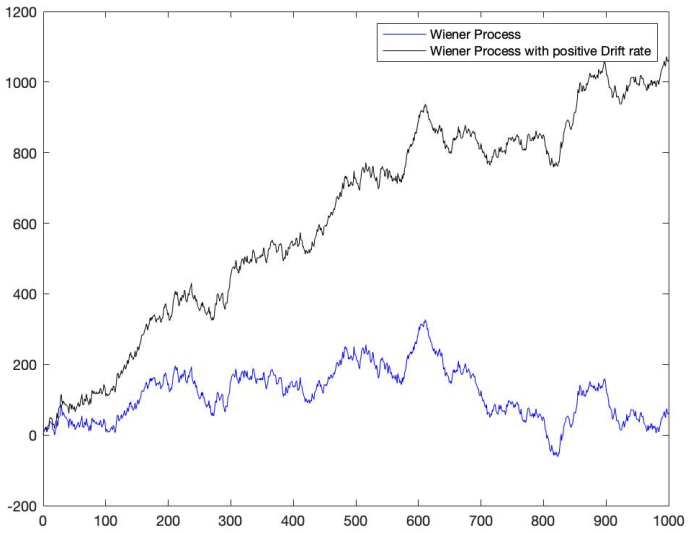

Figure 2.1: Wiener Process, own representation

Anyway, it is observable that the graph of the generalized Wiener Process can still fall below zero. We solve this issue in the next step.

2.3. Itô's Lemma

Itô (1951) build the basis for the valuation of financial derivatives. He replaced the constants a and b with functions that depend on the state variable x and time t. For the mathematical terms we can refer to Hull (2018), who summed up the needed adjustments to receive the final formula. In particular,

$$\boldsymbol{dx = a(x,t)dt + b(x,t)dz} \tag{2.2}$$

reflects the replacement with the functions $a(x,t)$ and $b(x,t)$. Next, a function f that follows an Itô Process itself is introduced, changing the function to

$$\boldsymbol{df = \left(\frac{\partial f}{\partial x}a + \frac{\partial f}{\partial t} + \frac{1}{2}\frac{\partial^2 f}{\partial x^2}b^2\right)dt + \frac{\partial f}{\partial x}b\,dz.} \tag{2.3}$$

This equation is known as Itô's lemma (Dixit & Pindyck, 1994). It allows the valuation of any financial derivative if applied to it. We can adjust the notation with $a(S,t) = \mu S$ and $b(S,t) = \sigma S$ to apply it to

the stock market. The drift rate, with μ being the rate of return, as well as the volatility, with σ being the standard deviation, are now noted in terms of the underlying stock price S. The prior equation then changes to

$$\boldsymbol{df = \left(\frac{\partial f}{\partial S}\mu S + \frac{\partial f}{\partial t} + \frac{1}{2}\frac{\partial^2 f}{\partial S^2}\sigma^2 S^2\right)dt + \frac{\partial f}{\partial S}\sigma S\, dz,} \tag{2.4}$$

where f depends on the stock price S and time t. Still, both f and S are subject to the same underlying uncertainty dz (Hull, 2018). At this point we need to come back to the not yet solved problem with possible negative stock values. To prove that the prior formula now adjusted to this problem, we replace f with $ln\ (S)$. Hence,

$$\boldsymbol{dlnS = \left(\mu - \frac{\sigma^2}{2}\right)dt + \sigma\, dz.} \tag{2.5}$$

The formula has, in contrast to the previous one, a constant rate of return μ and standard deviation σ. This concludes to the fact that lognormal values for S are normally distributed and, therefore, values for S are lognormally distributed. Since it implies a distribution that only contains values greater than zero, this fact is of great meaning for our work. We now have the certainty that the geometric Brownian motion is a suitable model to simulate the stock market.

2.4. Volatility Smile

The quality of an option pricing model depends on how well the model reflects the used parameters. Some parameters are easily observed, e.g. the option strike and value of the underlying are observable in the market. The volatility on the other hand is not observable. It needs to be estimated from other sources of data. Due to this uncertainty, Abken & Nandi (1996) even called the volatility one of the most important factors when it comes to the pricing of options. We need to understand how volatility behaves in different situations to be able to reflect the behavior in the parameters.

We can differentiate between historic and implied volatility. The historic volatility is estimated from past data and applied to future developments to predict their development. The implied volatility is a measure for future expected volatility and gained through the Black and Scholes (1973) and Merton (1973) Model (BSM) which will be explained later. Using a numerical process and inverting the BSM, we can calculate

values for the implied volatility of European options. Doing this for different strike prices K, we receive an interesting result. Since the volatility is not dependent on the strike price, we should observe a constant volatility. Anyhow, this is not the case. Heston (1993), Paul & Baschnagel (2013) and Mondal et al. (2017) proved this in their works. The volatility of a derivative depends on how far an option is in the money (ITM) or out of the money (OTM). Figure 2.2 shows the result, the so called volatility Smile.

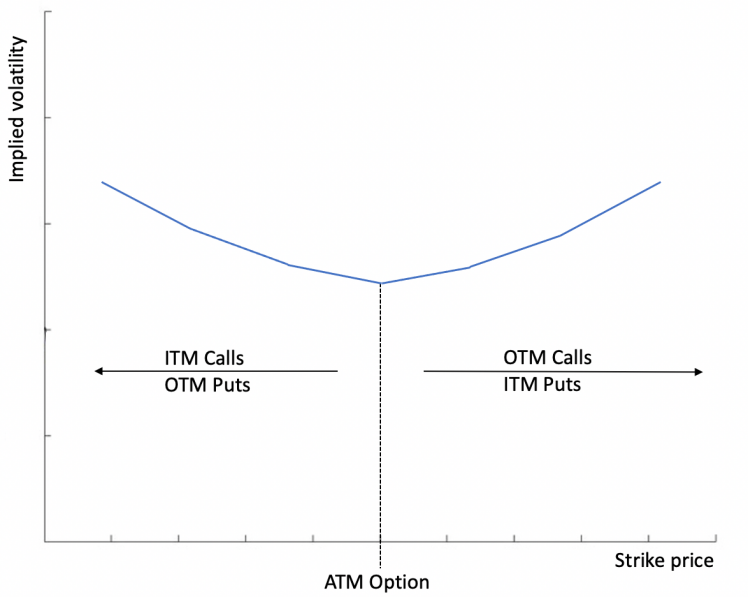

Figure 2.2: Volatility Smile, own representation

The further an option is ITM or OTM the higher the implied volatility for options. The volatility is the lowest when it is at the money (ATM). Concluding from this fact, the volatility is not constant for different states of options. This observation is of great meaning since it reveals why some option pricing models are weaker and some are stronger in terms of accuracy. The stronger ones can reflect this behavior in their process, while the weaker ones are not. How evident the differences are will be shown in the numerical part of this work.

3. Valuation Methods

3.1. Black-Scholes-Merton Model

As mentioned in the introduction, the correct valuation of options is of great meaning for the financial markets. Many attempts tried to improve option pricing models over the years. The first one delivering an accurate and reliable model were Black and Scholes (1973) and Merton (1973). With their BSM Model they introduced a full closed-form solution for the valuation of European options. It is built on seven assumptions that idealize the reality, namely

1. A constant risk-free interest rate is known.
2. The stock price follows a geometric Brownian motion.
3. The stock does not pay any dividends as in Black and Scholes (1973) or pays a continuous dividend yield as in Merton (1973).
4. It is a European option that can only be exercised at maturity.
5. There are no transaction costs when buying or selling the stock or the option.
6. Money can be borrowed or invested at the risk-free interest rate.
7. Short sales are possible.

I will omit an extensive derivation of the BSM formula since it is not the main subject of this work. Using a replication of a portfolio, the process is precisely explained in Hull (2018) and others. The solution for a call with a payoff of

$$\boldsymbol{C(S,T) = \max\{S_T - K, 0\}}, \tag{3.1}$$

is given by

$$\boldsymbol{C(S,t) = Se^{-q(T-t)}\phi(d_1) - Ke^{-r(T-t)}\phi(d_2)}, \tag{3.2}$$

with

$$\boldsymbol{d_1 = \frac{\ln\left(\frac{S}{K}\right) + (r - q + \frac{1}{2}\sigma^2)(T-t)}{\sigma\sqrt{T-t}}},$$

and

$$\boldsymbol{d_2 = d_1 - \sigma\sqrt{T-t}},$$

where ϕ stands for the cumulative normal distribution function, S is the spot price, K the strike price, r the risk-free rate, q the continuous dividend yield, σ the volatility, T the expiration time and t a certain point in time smaller than T. With the help of this formula, solutions for European call and put options can be calculated. Using the solution for the European call, we can determine the value for a European put option using the put-call parity

$$\boldsymbol{C + Ke^{-rT} = P + S_0 e^{-qT}} \tag{3.3}$$

by inserting all values and solving for *P.* The fact that the exercise of American call options is never optimal in the absence of dividends sets the American equal to the European option value. Only the value of American put options cannot be calculated with the BSM formula. For this case, different methods are needed. Moreover, if q > 0 both American calls and puts require other pricing tools.

3.2. Cox-Ross-Rubinstein Method

One of these methods is the binomial tree introduced by Cox et al. (1979). It can be used to calculate the value of both, European and American options. We briefly describe this model since it is one of the basic models and is able to deliver values of good quality. Therefore, a comparison between the Cox-Ross-Rubinstein (CRR) Model and the Heston Model can be used to evaluate the latter one.

The model assumes that the price of an option can only move to two different states. The process is divided into two steps: the calculation of the underlying value going forward in time and the recursive calculation of the options going back in time. For both ways we use increments of $\Delta t = \frac{(T-t)}{n}$. The underlying can either increase by the factor

$$\boldsymbol{u = e^{\sigma\sqrt{\Delta t}}} \tag{3.4}$$

or decrease by the factor

$$\boldsymbol{d = e^{-\sigma\sqrt{\Delta t}} = \frac{1}{u}.} \tag{3.5}$$

To avoid any arbitrage opportunities, *u > r > d* must hold, where *r* is the risk-free rate. These values are used to calculate the risk-free probability

$$\boldsymbol{p = \frac{e^{r\Delta t} - d}{u - d}}. \tag{3.6}$$

Following Cox et al. (1979), we start with the calculation of the underlying, creating a binomial grid consisting of

$$\boldsymbol{S_{i,j} = S_{0,0} u^j d^{i-j}} \tag{3.7}$$

for *i=0,1,…,n* and *j=0,1,…,i* with i representing the time period and j the number of up moves. Afterwards, the option values for the maturity are calculated, using

$$\boldsymbol{C_{n,j} = max\{0, K - S_{n,j}\}} \tag{3.8}$$

for call options. From here on, all other option values can be calculated using

$$\boldsymbol{C_{i,j} = e^{-r\Delta t}\left[pC_{i+1,j+1} + (1-p)C_{i+1,j}\right]}. \tag{3.9}$$

The same process is applicable for American options as well, except that the early exercise component has to be implemented in formula 3.9, resulting in

$$\boldsymbol{C_{i,j} = max\{K - S_{n,j}, e^{-r\Delta t}\left[pC_{i+1,j+1} + (1-p)C_{i+1,j}\right]\}}. \tag{3.10}$$

4. Heston stochastic volatility Model

4.1. The Heston Model

4.1.1. Stochastic Process of the Heston Model

After explaining the theoretic basis, we will now focus on the main model of this work. The Heston Model combines the knowledge about stochastic processes and the behavior of volatility explained in chapter 2. While the prior explained models use a constant volatility, the Heston Model replaces this assumption with a stochastic process that simulates the volatility, which in that case depends on a random walk as well. Therefore, the model is supposed to replicate the actual market conditions in a more precise way and is able to deliver more accurate option valuations. Heston (1993) assumes in his publication that the underlying follows a log-normal distribution. The used process is the one underlying the Black-Scholes valuation, while the volatility follows the Cox-Ingersoll-Ross (CIR) (1985) Model.

The CIR Model is an extension of the Vasicek (1977) Model. Both are one factor models that can be used to replicate the evolution of interest rates due to the mean reversion property. The Vasicek Model is described by

$$\boldsymbol{dr = a(b - r)dt + \sigma dW,} \tag{4.1}$$

where *r* is the interest rate, *a* is the speed reversion, *b* is the long term mean level, σ is the volatility of the interest rate and *dW* is the Wiener Process we already introduced. The CIR adds a square root to avoid negative interest rate values. This leads to

$$\boldsymbol{dr = a(b - r)dt + \sigma\sqrt{r}dW}. \tag{4.2}$$

Summed up we receive a bivariate system of stochastic differential equations with

$$\boldsymbol{dS = \mu Sdt + \sqrt{v}SdW_1} \tag{4.3}$$

for the underlying and

$$\boldsymbol{dv = \kappa(\Theta - v)dt + \sigma\sqrt{v}dW_2} \tag{4.4}$$

for the variance *v*, being formula (4.2) with different notion. We have to note here, that, if κ is greater than zero, v_t will not be negative. Moreover, Cox et al. (1985) show, under the constraint of $2\kappa\theta \geq \sigma^2$, v_t will be almost strictly positive (Nagel, 2001). This constraint is also known as the Feller condition.

4.1.2. Risk neutral adjustments

For the next step it is important to note that the volatility $\sqrt{v}$ is only indirectly modeled in the Heston Model via the variance v. To do so, we need the Ornstein-Uhlenbeck Process, which describes the underlying process for the volatility *h* = $\sqrt{v}$ as

$$\boldsymbol{dh_t = -\beta h_t + \delta dz_2}. \tag{4.5}$$

Now we apply Itô's lemma to $v_t = h_t^2$ which results in

$$\boldsymbol{dv_t = \left(\delta^2 - 2\beta v_t\right)dt + 2\delta\sqrt{v_t}dz_2}. \tag{4.6}$$

Here we can define $\kappa = 2\beta,\ \theta = \frac{\delta^2}{2\beta}$ and $\sigma = 2\delta$. In doing so, we receive the same formula for dv_t as we did in equation (4.4). Moreover, we need to make another adjustment to the process. The asset as well as the variance follow the process in equation (4.1), respectively (4.2), under the historical measure $\mathbb{P}$. Since we are pricing assets, the fundamental theorem of asset pricing holds, including the absence of arbitrage and resulting in a risk neutral measurement. Therefore, in this case, we have to use the risk neutral measure $\mathbb{Q}$. For the transformation we are applying the Girsanov's theorem to the stochastic differential equations (4.3) and (4.4). Afterwards, the risk neutral stock price is defined as

$$\boldsymbol{dS_t = rS_t dt + \sqrt{v_t} S_t\, dW'_1}, \tag{4.7}$$

where

$$\boldsymbol{dW'_1 = \left(dW_1 + \frac{\mu - r}{\sqrt{v_t}} t\right)}.$$

To obtain the risk neutral function for the variance, we need to introduce a function for the drift of dv. This function is expressed by $\lambda(S_t, v_t, t)$ and is called the volatility risk premium. This results in a risk neutral process for the variance expressed by

$$\boldsymbol{dv_t = [\kappa(\theta - v_t) - \lambda(S_t, v_t, t)]dt + \sigma\sqrt{v_t}\, dW'_2,} \tag{4.8}$$

where

$$\boldsymbol{dW'_2 = \left(dW_2 + \frac{\lambda(S_t, v_t, t)}{\sigma\sqrt{v_t}} t\right).}$$

The final step for the adjustment is explained in Heston (1993). Since Breeden's (1979) consumption model yields a premium proportional to the variance, $\lambda(S_t, v_t, t) = \lambda v_t$, where λ is a constant. If we substitute this for λv_t in equation (4.8), the final risk neutral process for the variance is

$$\boldsymbol{dv_t = \kappa^*(\theta^* - v_t)dt + \sigma\sqrt{v_t}\, dW'_2,} \tag{4.9}$$

where $\kappa^* = \kappa + \lambda$ and $\theta^* = \frac{\kappa\theta}{\kappa+\lambda}$ are now risk neutral parameters. As a final note to the adjustment we can observe, that if $\lambda = 0$, κ^* and θ^* equal κ and θ. This way, the risk neutral measure $\mathbb{Q}$ and the physical measure $\mathbb{P}$ are the same (Rouah, 2013). Since this thesis only deals with risk neutral option valuation, λ will be set to zero in all cases. Therefore, the asterisk in the parameters and the apostrophe for notation of the Brownian motion will be omitted.

4.1.3. Derivation of the Heston PDE

The approach for the derivation of the Heston PDE is the same as for the Black-Scholes Partial-Differential-Equation (PDE) (Black and Scholes, 1973). For the derivation of the Black-Scholes PDE, a portfolio consisting of the underlying asset and one derivative to hedge the underlying is formed. To derive the Heston PDE, a second derivative is needed to hedge the volatility as well. Hence, we create a portfolio consisting of one option $V = V(S, v, t)$, Δ units of the stock, and φ units of the other option $U = U(S, v, t)$. For simplicity the subscripts of *t* will be omitted. The value of the created portfolio is expressed by

$$\boldsymbol{\Pi = V + \Delta S + \varphi U.} \tag{4.10}$$

The change of the portfolio is expressed by

$$\mathbf{d\Pi} = \boldsymbol{dV} + \Delta \boldsymbol{dS} + \boldsymbol{\varphi dU}. \tag{4.11}$$

As it is done for the Black-Scholes PDE as well, we now apply Itô's lemma to the derivatives *V* and *U*. Starting with V, we need to differentiate V with respect to the variables t, S and v and form a second order Taylor series expansion. As a result, the process of dV follows

$$\boldsymbol{dV} = \frac{\boldsymbol{\partial V}}{\boldsymbol{\partial t}}\boldsymbol{dt} + \frac{\boldsymbol{\partial V}}{\boldsymbol{\partial S}}\boldsymbol{dS} + \frac{\boldsymbol{\partial V}}{\boldsymbol{\partial v}}\boldsymbol{dv} + \frac{\mathbf{1}}{\mathbf{2}}\boldsymbol{vS^2}\frac{\boldsymbol{\partial^2 V}}{\boldsymbol{\partial S^2}}\boldsymbol{dt} + \frac{\mathbf{1}}{\mathbf{2}}\boldsymbol{v\sigma^2}\frac{\boldsymbol{\partial^2 V}}{\boldsymbol{\partial v^2}}\boldsymbol{dt} + \boldsymbol{\sigma\rho vS}\frac{\boldsymbol{\partial^2 V}}{\boldsymbol{\partial S \partial v}}\boldsymbol{dt}. \tag{4.12}$$

This is not the instant result, but the equation that appears after implementing following rearrangements:

$$\begin{gathered}
(\boldsymbol{dS})^{\mathbf{2}} = \boldsymbol{vS^2}(\boldsymbol{dz_1})^{\mathbf{2}} = \boldsymbol{vS^2 dt}, \\
(\boldsymbol{dv})^{\mathbf{2}} = \boldsymbol{\sigma^2 v dt}, \\
\boldsymbol{dS dv} = \boldsymbol{\sigma v S dz_1 dz_2} = \boldsymbol{\sigma\rho v S dt}, \\
(\boldsymbol{dt})^{\mathbf{2}} = \mathbf{0}, \\
\boldsymbol{dz_1 dt} = \boldsymbol{dz_2 dt} = \mathbf{0}.
\end{gathered} \tag{4.13}$$

Continuing with *U,* we apply the same adjustments as we did for *V*. Since the notation is equal to equation (4.12), but in terms of *U,* we are omitting it. Inserting the two Taylor series expansion into (4.11), we receive

$$\begin{aligned}
\mathbf{d\Pi} = & \left[\frac{\boldsymbol{\partial V}}{\boldsymbol{\partial t}} + \frac{\mathbf{1}}{\mathbf{2}}\boldsymbol{vS^2}\frac{\boldsymbol{\partial^2 V}}{\boldsymbol{\partial S^2}} + \boldsymbol{\sigma\rho vS}\frac{\boldsymbol{\partial^2 V}}{\boldsymbol{\partial S \partial v}} + \frac{\mathbf{1}}{\mathbf{2}}\boldsymbol{v\sigma^2}\frac{\boldsymbol{\partial^2 V}}{\boldsymbol{\partial v^2}}\right]\boldsymbol{dt} \\
& + \boldsymbol{\varphi}\left[\frac{\boldsymbol{\partial U}}{\boldsymbol{\partial t}} + \frac{\mathbf{1}}{\mathbf{2}}\boldsymbol{vS^2}\frac{\boldsymbol{\partial^2 U}}{\boldsymbol{\partial S^2}} + \boldsymbol{\sigma\rho vS}\frac{\boldsymbol{\partial^2 U}}{\boldsymbol{\partial S \partial v}} + \frac{\mathbf{1}}{\mathbf{2}}\boldsymbol{v\sigma^2}\frac{\boldsymbol{\partial^2 U}}{\boldsymbol{\partial v^2}}\right]\boldsymbol{dt} \\
& + \left[\frac{\boldsymbol{\partial V}}{\boldsymbol{\partial S}} + \boldsymbol{\varphi}\,\frac{\boldsymbol{\partial U}}{\boldsymbol{\partial S}} + \Delta\right]\boldsymbol{dS} + \left[\frac{\boldsymbol{\partial V}}{\boldsymbol{\partial v}} + \boldsymbol{\varphi}\frac{\boldsymbol{\partial U}}{\boldsymbol{\partial v}}\right]\boldsymbol{dv}
\end{aligned} \tag{4.14}$$

for the portfolio composition. At this point, the portfolio is still carrying a risk. Therefore, the number of units Δ for the stocks and φ for the volatility need to be adjusted. To represent a riskless portfolio, the hedge parameters need to be set to

$$\boldsymbol{\varphi} = -\frac{\boldsymbol{\partial V}}{\boldsymbol{\partial v}} \Big/ \frac{\boldsymbol{\partial U}}{\boldsymbol{\partial v}} \tag{4.15}$$

and

$$\Delta = -\boldsymbol{\varphi}\,\frac{\boldsymbol{\partial U}}{\boldsymbol{\partial S}} - \frac{\boldsymbol{\partial V}}{\boldsymbol{\partial S}}.$$

This way the last two terms of equation (4.14) are set to 0, meaning neither movements in stocks nor in volatility effect the portfolio value anymore (Rouah, 2013 and Mondal et al., 2017). Having a riskless portfolio, we know that the portfolio must earn the risk-free interest rate *r*, given fundamental portfolio theory. Consequently, equation (4.11) changes to

$$\mathbf{d\Pi} = \boldsymbol{r}(\boldsymbol{V} + \Delta\boldsymbol{S} + \boldsymbol{\varphi U})\boldsymbol{dt}. \tag{4.16}$$

If we now equate equations (4.14) and (4.16), drop the dt term, substitute the hedging parameters and re-arrange everything, we obtain

$$\frac{\left[\frac{\boldsymbol{\partial V}}{\boldsymbol{\partial t}} + \frac{\mathbf{1}}{\mathbf{2}}\boldsymbol{vS^2}\frac{\boldsymbol{\partial^2 V}}{\boldsymbol{\partial S^2}} + \boldsymbol{\sigma\rho vS}\frac{\boldsymbol{\partial^2 V}}{\boldsymbol{\partial S\partial v}} + \frac{\mathbf{1}}{\mathbf{2}}\boldsymbol{v\sigma^2}\frac{\boldsymbol{\partial^2 V}}{\boldsymbol{\partial v^2}}\right] - \boldsymbol{rV} + \boldsymbol{rS}\frac{\boldsymbol{\partial V}}{\boldsymbol{\partial S}}}{\frac{\boldsymbol{\partial V}}{\boldsymbol{\partial v}}} = \frac{\left[\frac{\boldsymbol{\partial U}}{\boldsymbol{\partial t}} + \frac{\mathbf{1}}{\mathbf{2}}\boldsymbol{vS^2}\frac{\boldsymbol{\partial^2 U}}{\boldsymbol{\partial S^2}} + \boldsymbol{\sigma\rho vS}\frac{\boldsymbol{\partial^2 U}}{\boldsymbol{\partial S\partial v}} + \frac{\mathbf{1}}{\mathbf{2}}\boldsymbol{v\sigma^2}\frac{\boldsymbol{\partial^2 U}}{\boldsymbol{\partial v^2}}\right] - \boldsymbol{rU} + \boldsymbol{rS}\frac{\boldsymbol{\partial U}}{\boldsymbol{\partial S}}}{\frac{\boldsymbol{\partial U}}{\boldsymbol{\partial v}}}. \tag{4.17}$$

In this equation we have the same function twice, except the fact that the left-hand side is a function of *V* and the right-hand side is a function of *U*. As Heston (1993) shows, it is possible to rewrite and define the function as

$$\boldsymbol{f}(\boldsymbol{S},\boldsymbol{v},\boldsymbol{t}) = -\boldsymbol{\kappa}(\boldsymbol{\theta}-\boldsymbol{v}) + \boldsymbol{\lambda}(\boldsymbol{S},\boldsymbol{v},\boldsymbol{t}) \tag{4.18}$$

where $\lambda(S, v, t)$ is again the risk premium of the volatility. In chapter 4.1.2, we already learned about Breeden's (1979) consumption model $\lambda(S, v, t) = \lambda v$, where λ is a constant. We use this again on the left-hand side of equation (4.18) and rearrange it. The result is

$$\frac{\partial U}{\partial t} + \frac{1}{2} v S^2 \frac{\partial^2 U}{\partial S^2} + \sigma \rho v S \frac{\partial^2 U}{\partial S \partial v} + \frac{1}{2} v \sigma^2 \frac{\partial^2 U}{\partial v^2} - rU + rS \frac{\partial U}{\partial S} + [\kappa(\theta - v) + \lambda(S, v, t)] \frac{\partial U}{\partial v} = 0. \tag{4.19}$$

In a further step, we can set up boundary conditions for a European Call option

$$U(S, v, T) = \max(0, S_T - K) \tag{4.20}$$

with strike price *K* and maturity *T*. There are three boundaries: The stock price equals zero then the call price equals zero as well. The stock price striving towards infinity, where the option delta equals one, and the volatility striving towards infinity, where the call option price equals the stock price. Summed up, the boundaries are

$$\begin{aligned} U(0, v, t) &= 0, \\ \frac{\partial U}{\partial S}(\infty, v, t) &= 1 \end{aligned} \tag{4.21}$$

and

$$U(S, \infty, t) = S.$$

If we consider these boundaries in equation (4.19), we can rewrite it and obtain

$$\frac{\partial U}{\partial t} + \mathcal{A}U - rU = 0, \tag{4.22}$$

where

$$\mathcal{A} = rS \frac{\partial}{\partial S} + \frac{1}{2} v S^2 \frac{\partial^2}{\partial S^2} + [\kappa(\theta - v) + \lambda(S, v, t)] \frac{\partial}{\partial v} + \frac{1}{2} v \sigma^2 \frac{\partial^2}{\partial v^2} + \sigma \rho v S \frac{\partial^2}{\partial S \partial v},$$

which is also called the generator of the Heston Model. As Mondal et al. (2017) state, the first part of equation (4.22) is the generator of the Black-Scholes Model, while the second part extends the PDE for stochastic volatility needed for the Heston Model.

For financial derivatives, it is very common to express stock prices in logarithmic terms since stock prices are often log normally distributed Hull (2018). This assumption is made for the Black-Scholes Model as well. Therefore, we define *x=ln(S)* as in Heston (1993). If we apply this to the Heston PDE and express it in terms of (x, v, t), the PDE is no longer depending on *S*, but on *x.* To realize this, we firstly need to derive the derivatives for

$$\frac{\partial U}{\partial S} = \frac{\partial U}{\partial x}\frac{1}{S}, \qquad \frac{\partial^2 U}{\partial v \partial S} = \frac{\partial}{\partial v}\left(\frac{1}{S}\frac{\partial U}{\partial x}\right) = \frac{1}{S}\frac{\partial^2 U}{\partial v \partial x} \tag{4.23}$$

and

$$\frac{\partial^2 U}{\partial S^2} = \frac{\partial}{\partial S}\left(\frac{1}{S}\frac{\partial U}{\partial x}\right) = -\frac{1}{S^2}\frac{\partial U}{\partial x} + \frac{1}{S}\frac{\partial^2 U}{\partial S \partial x} = -\frac{1}{S^2}\frac{\partial U}{\partial x} + \frac{1}{S^2}\frac{\partial^2 U}{\partial x^2},$$

using the chain rule and the product role, respectively. Substituting these terms as well as *λ(S,v,t)=λv* from Breeden's (1979) consumption model into the Heston PDE, we obtain the Heston PDE in terms of *x*, that is

$$\frac{\partial U}{\partial t} + \frac{1}{2}v\frac{\partial^2 U}{\partial x^2} + \left(r - \frac{1}{2}v\right)\frac{\partial U}{\partial x} + \sigma\rho v\frac{\partial^2 U}{\partial v \partial x} + \frac{1}{2}v\sigma^2\frac{\partial^2 U}{\partial v^2} - rU + [\kappa(\theta - v) + \lambda v]\frac{\partial U}{\partial v} = 0. \tag{4.24}$$

4.1.4. PDE for P1 and P2

To derive the PDE for the Probabilities $P_1 = \mathbb{Q}^S(S_T > K)$ and $P_2 = \mathbb{Q}(S_T > K)$, we start with the payoff of a call option that is similar to what Black and Scholes (1973) present, being

$$C(K) = S_t P1 - Ke^{-r\tau}P2. \tag{4.25}$$

Replacing *x=ln(S),* we receive

$$\boldsymbol{C(K) = e^x P1 - Ke^{-r\tau} P2.} \tag{4.26}$$

The PDE in (4.24) can now be satisfied by this equation for the derivative, formerly noted by *U*. Therefore, we need to derive the required derivatives and substitute them into the PDE. The derivative with respect to *t* is represented by

$$\boldsymbol{\frac{\partial C}{\partial t} = e^x \frac{\partial P_1}{\partial t} - Ke^{-r\tau}\left[rP_2 + \frac{\partial P_2}{\partial t}\right],} \tag{4.27}$$

with respect to x by

$$\boldsymbol{\frac{\partial C}{\partial x} = e^x \left[P_1 + \frac{\partial P_1}{\partial x}\right] - Ke^{-r\tau}\frac{\partial P_2}{\partial x},} \tag{4.28}$$

with respect to x^2 by

$$\begin{aligned} \boldsymbol{\frac{\partial^2 C}{\partial x^2}} &= \boldsymbol{e^x P_1 + 2e^x \frac{\partial P_1}{\partial x} + e^x \frac{\partial^2 P_1}{\partial x^2} - Ke^{-r\tau}\frac{\partial^2 P_2}{\partial x^2}} \\ &= \boldsymbol{e^x \left[P_1 + 2\frac{\partial P_1}{\partial x} + \frac{\partial^2 P_1}{\partial x^2}\right] - Ke^{-r\tau}\frac{\partial^2 P_2}{\partial x^2},} \end{aligned} \tag{4.29}$$

with respect to v by

$$\boldsymbol{\frac{\partial C}{\partial v} = e^x \frac{\partial P_1}{\partial v} - Ke^{-r\tau}\frac{\partial P_2}{\partial v},} \tag{4.30}$$

with respect to v^2 by

$$\boldsymbol{\frac{\partial^2 C}{\partial v^2} = e^x \frac{\partial^2 P_1}{\partial v^2} - Ke^{-r\tau}\frac{\partial^2 P_2}{\partial v^2},} \tag{4.31}$$

and with respect to x and v by

$$\boldsymbol{\frac{\partial^2 C}{\partial x \partial v} = e^x \left[\frac{\partial P_1}{\partial v} + \frac{\partial^2 P_1}{\partial x \partial v}\right] - Ke^{-r\tau}\frac{\partial^2 P_2}{\partial v^2}.} \tag{4.32}$$

Using the mentioned fact that *C(K)* satisfies the PDE (4.24), we can now replace *U* by *C*. The result is

$$\frac{\partial C}{\partial t} = \frac{1}{2} v \frac{\partial^2 C}{\partial x^2} + \left(r - \frac{1}{2} v\right) \frac{\partial C}{\partial x} + \sigma \rho v \frac{\partial^2 C}{\partial v \partial x} + \frac{1}{2} v \sigma^2 \frac{\partial^2 C}{\partial v^2} - rC + [\kappa(\theta - v) - \lambda v] \frac{\partial C}{\partial v} = 0. \tag{4.33}$$

Before obtaining the PDEs for P1 and P2 out of this equation, it is necessary to be assured that it holds for any contractual features of *C(K).* Heston (1993) delivers the proof for it by showing that for every *r>0* and *K=0* and *S=1*, the call price is simply P1. Also, for *K=1, S=0* and *r=0,* he shows that the call price is simply -P2, and therefore -P2 as well as P2 follow the PDE. Now we can place the derivatives (4.27) – (4.32) in the PDE (4.33). Regrouping the terms evenly to P1 and getting rid of e^x afterwards, we obtain the Heston PDE for P1, which is

$$\frac{\partial P_1}{\partial t} + \frac{1}{2} v \left[P_1 + 2 \frac{\partial P_1}{\partial x} + \frac{\partial^2 P_1}{\partial x^2}\right] + \left(r - \frac{1}{2} v\right) \left[P_1 + \frac{\partial P_1}{\partial x}\right] + \sigma \rho v \left[\frac{\partial P_1}{\partial v} + \frac{\partial^2 P_1}{\partial x \partial v}\right] + \frac{1}{2} v \sigma^2 \frac{\partial^2 P_1}{\partial v^2} - rP_1 + [\kappa(\theta - v) - \lambda v] \frac{\partial P_1}{\partial v} = 0. \tag{4.34}$$

By rearranging, we obtain

$$\frac{\partial P_1}{\partial t} + \left(r + \frac{1}{2} v\right) \frac{\partial P_1}{\partial x} + \frac{1}{2} v \frac{\partial^2 P_1}{\partial x^2} + \sigma \rho v \frac{\partial^2 P_1}{\partial v \partial x} + [\sigma \rho v + \kappa(\theta - v) - \lambda v] \frac{\partial P_1}{\partial v} + \frac{1}{2} v \sigma^2 \frac{\partial^2 P_1}{\partial v^2} = 0. \tag{4.35}$$

In a next step, we repeat the procedure to obtain the PDE for P2. We Regroup the terms of the derivatives (4.27) – (4.32) evenly to P2, but this time cancel $-Ke^{-r\tau}$ out. After placing everything in the PDE (4.33), we get

$$\frac{\partial P_2}{\partial t} + \frac{1}{2} v \frac{\partial^2 P_2}{\partial x^2} + \left(r - \frac{1}{2} v\right) \frac{\partial P_2}{\partial x} + \sigma \rho v \frac{\partial^2 P_2}{\partial v \partial x} + \frac{1}{2} v \sigma^2 \frac{\partial^2 P_2}{\partial v^2} + [\kappa(\theta - v) - \lambda v] \frac{\partial P_2}{\partial v} = 0. \tag{4.36}$$

Combining (4.35) and (4.36), we have

$$\frac{\partial P_j}{\partial t} + \sigma\rho v\frac{\partial^2 P_j}{\partial v \partial x} + \frac{1}{2}v\frac{\partial^2 P_j}{\partial x^2} + \frac{1}{2}v\sigma^2\frac{\partial^2 P_j}{\partial v^2} + (r + u_j v)\frac{\partial P_j}{\partial x} + (a - b_j v)\frac{\partial P_j}{\partial v} = 0, \tag{4.37}$$

for $j = 1,2$, and where $u_1 = \frac{1}{2}$; $u_2 = -\frac{1}{2}$; $a = \kappa\theta$; $b_1 = \kappa + \lambda - \rho\sigma$; $b_2 = \kappa + \lambda$.

4.1.5. Characteristic function

Each stochastic volatility model has a unique characteristic function $f_j(\phi;x,v)$, that completely describes the models probability distribution. Knowing the characteristic function allows us to recovery each in-the-money probability P_j via the Gil-Pelaez (1951) inversion theorem as

$$P_j = \Pr(lnS_T > lnK) = \frac{1}{2} + \frac{1}{\pi}\int_0^\infty Re\left[\frac{e^{-i\phi lnK} f_j(\phi; x, v)}{i\phi}\right] d\phi. \tag{4.38}$$

At maturity, the probabilities are bounded by the terminal condition

$$P_j = 1_{X_T > lnK}, \tag{4.39}$$

where 1 is the indicator function (Heston, 1993; Rouah, 2013). It says that if $S_T > K$, the probability that the call option is in the money is equal to one. Returning to logarithmic stock prices, Heston (1993) postulates a characteristic function for $x=ln(S)$ of the form

$$f_j(\phi; x, v) = exp\left(C_j(\tau, \phi) + D_j(\tau, \phi)v_t + i\phi x_t\right), \tag{4.40}$$

where $i = \sqrt{-1}$ is an imaginary unit, $\tau = T - t$ is the time to maturity and C_j and D_j are coefficients. At this point, we need to use Feynman-Kac theorem to show that the function will also follow the PDE (4.37). The theorem prescribes that if a function $f(x_t, t)$ of the Heston bivariate system of SDEs $x_t = (x_t, v_t) = (lnS_t, v_t)$ satisfies the PDE

$$\frac{\partial f}{\partial t} - rf + \mathcal{A}f = 0, \tag{4.41}$$

where $\mathcal{A}$ is the Heston generator from equation (4.22), the solution to that function is the conditional expectation

$$\boldsymbol{f(x_t, t) = E[f(x_T, T)|\mathcal{F}_t]}. \tag{4.42}$$

Setting $f(x_t, t) = \exp(i\phi ln S_T)$, we get the solution

$$\boldsymbol{f(x_t, t) = E\left[e^{i\phi ln S_T}|x_t, v_t\right]}. \tag{4.43}$$

This is the characteristic function for $x_T = lnS_T$. Finally, we can see that the function f_j follows the PDE (4.37) as

$$\begin{aligned} -\frac{\partial f_j}{\partial \tau} + \sigma\rho v\frac{\partial^2 f_j}{\partial v \partial x} + \frac{1}{2}v\frac{\partial^2 f_j}{\partial x^2} + \frac{1}{2}v\sigma^2\frac{\partial^2 f_j}{\partial v^2} \\ +\left(r + u_j v\right)\frac{\partial f_j}{\partial x} + \left(a - b_j v\right)\frac{\partial f_j}{\partial v} = 0. \end{aligned} \tag{4.44}$$

as we stated before. Compared to the PDE (4.37), this PDE for the first time has a negative sign in front, since we no longer use t, but τ. As we already did for PDE (4.24), we need to derive several derivations included in PDE (4.44), so we can evaluate it. The needed derivations are

$$\begin{aligned} \frac{\partial f_j}{\partial \tau} &= \left(\frac{\partial C_j}{\partial \tau} + \frac{\partial D_j}{\partial \tau}v\right) f_j, \\ \frac{\partial f_j}{\partial x} = i\phi f_j, \qquad \frac{\partial f_j}{\partial x} &= D_j f_j, \\ \frac{\partial^2 f_j}{\partial x^2} &= -\phi^2 f_j, \\ \frac{\partial^2 f_j}{\partial v^2} &= {D_j}^2 f_j, \end{aligned} \tag{4.45}$$

and

$$\frac{\partial^2 f_j}{\partial v \partial x} = i\phi D_j f_j.$$

Inserting everything into (4.44), we can get rid of f_j and obtain

$$-\left(\frac{\partial C_j}{\partial \tau}+\frac{\partial D_j}{\partial \tau}v\right)+\sigma\rho v i\phi D_j-\frac{1}{2}v\phi^2+\frac{1}{2}v\sigma^2{D_j}^2 +\left(r+u_j v\right)i\phi+\left(a-b_j v\right)D_j=0. \tag{4.46}$$

This equation again contains two derivates, namely

$$\frac{\partial D_j}{\partial \tau}=\ \sigma\rho i\phi D_j-\frac{1}{2}\phi^2+\frac{1}{2}\sigma^2{D_j}^2+u_j i\phi-b_j D_j \tag{4.47}$$

and

$$\frac{\partial C_j}{\partial \tau}=ri\phi+aD_j. \tag{4.48}$$

Equation (4.47) is a Riccati equation in D_j, to be solved in the next subsection. Equation (4.48) is an ordinary derivative of C_j, that can easily be solved once D_j is obtained. To solve these equations, two initial conditions are needed. We know that the value of $x_T = lnS_T$ at. maturity $(\tau = 0)$ is known. Therefore, we can omit the expectation in the in (4.40) mentioned characteristic function

$$f_j(\phi; x, v) = exp\left(C_j(\tau,\phi)+D_j(\tau,\phi)v_t+i\phi x_t\right), \tag{4.49}$$

leaving only $\exp(i\phi x_t)$. Mathematically speaking, $D_j(0,\phi)=0$ and $C_j(0,\phi)=0$, being our two initial conditions to solve the Riccati equation.

4.1.6. Riccati Equation

A Riccati equation is a specific class of differential equation of the form

$$\frac{\partial y}{\partial x}=f(x)y^2(x)+g(x)y(x)+h(x). \tag{4.50}$$

Mikhailov & Nögel (2004) and Rouah (2013) show that we can rewrite equation (4.47) as the Heston Riccati equation of the form

$$\frac{\partial D_j}{\partial \tau} = P_j - Q_i D_j + R{D_j}^2 \tag{4.51}$$

where

$$P_j = u_j i\phi - \frac{1}{2}\phi^2,$$

$$Q_j = b_j - \sigma\rho i\phi,$$

$$R = \frac{1}{2}\sigma^2.$$

This equation can be solved by using the corresponding second-order ordinary differential equation (ODE)

$$w'' + Q_j w' + P_j R w = 0 \tag{4.52}$$

so that the solution for D_j is

$$D_j = -\frac{1}{R}\frac{w'}{w}. \tag{4.53}$$

The ODE itself then can be solved via the auxiliary equation $r^2 + Q_j r + P_j R = 0$. The two roots of this equation are

$$\alpha_j = \frac{-Q_j + \sqrt{{Q_i}^2 - 4P_j R}}{2} = \frac{-Q_j + d_j}{2} \tag{4.54}$$

and

$$\beta_j = \frac{-Q_j - \sqrt{{Q_j}^2 - 4P_j R}}{2} = \frac{-Q_j - d_j}{2}. \tag{4.55}$$

where

$$\boldsymbol{d_j = \alpha_j - \beta_j = \sqrt{Q_j{}^2 - 4P_jR} = \sqrt{(\sigma\rho i\phi - b_j)^2 - \sigma^2(2u_j i\phi - \phi^2)}.}$$

Keeping on with the Riccati formula, the solution for the Heston Riccati equation is given by

$$\boldsymbol{D_j = -\frac{1}{R}\frac{w'}{w} = -\frac{1}{R}\left(\frac{M\alpha e^{\alpha\tau} + N\beta e^{\beta\tau}}{Me^{\alpha\tau} + Ne^{\beta\tau}}\right) = -\frac{1}{R}\left(\frac{K\alpha e^{\alpha\tau} + \beta e^{\beta\tau}}{Ke^{\alpha\tau} + e^{\beta\tau}}\right),} \tag{4.56}$$

where now $K = M/N$. Recalling the initial condition $D_j(0, \phi) = 0$, we need to set $\tau = 0$ here as well. Doing so in the numerator of equation (4.56), we obtain $K\alpha + \beta = 0$ and following $K = -\beta/\alpha$. Placing these into equation (4.56) leads to

$$\boldsymbol{D_j = -\frac{\beta}{R}\left(\frac{-e^{\alpha\tau} + e^{\beta\tau}}{-g_j e^{\alpha\tau} + e^{\beta\tau}}\right) = -\frac{\beta}{R}\left(\frac{1 - e^{d_j\tau}}{1 - g_j e^{d_j\tau}}\right) = \frac{Q_j + d_j}{2R}\left(\frac{1 - e^{d_j\tau}}{1 - g_j e^{d_j\tau}}\right),} \tag{4.57}$$

where

$$\boldsymbol{g_j = -K = \frac{\beta}{\alpha} = \frac{b_j - \sigma\rho i\phi + d_j}{b_j - \sigma\rho i\phi - d_j} = \frac{Q_j - d_j}{Q_j + d_j}.}$$

Replacing $\beta = b_j - \sigma\rho i\phi + d_j$ and $R = \frac{1}{2}\sigma^2$ in this equation, we get

$$\boldsymbol{D_j(\tau, \phi) = \frac{b_j - \sigma\rho i\phi + d_j}{\sigma^2}\left(\frac{1 - e^{d_j\tau}}{1 - g_j e^{d_j\tau}}\right)} \tag{4.58}$$

as a result for D_j. We use this solution to obtain a solution von C_j as well. Therefore, we integrate equation (4.48), which has the form of

$$\boldsymbol{C_j = \int_0^\tau r\, i\phi dy + a\left(\frac{Q_j + d_j}{\sigma^2}\right)\int_0^\tau \left(\frac{1 - e^{d_j\tau}}{1 - g_j e^{d_j\tau}}\right)dy + K_1,} \tag{4.59}$$

where K_1 is a constant (Mikhailov & Nögel 2004). The other two terms of the equation can be solved separately. The first one term is easily obtained by $ri\phi\tau$, while the second integral is more difficult to solve.

It has to be found by substitution. Hence, we use $x = \exp(d_j y)$, which brings $dx = d_j \exp(d_j y)\, dy$ and $dy = dx/(x d_j)$. Rewriting equation (4.59) results in

$$\boldsymbol{C_j = ri\phi\tau + \frac{a}{d_j}\left(\frac{Q_j + d_j}{\sigma^2}\right)\int_1^{\exp(d_j\tau)}\left(\frac{1-x}{1-g_j x}\right)\frac{1}{x}dx + K_1}. \tag{4.60}$$

Afterwards, we can calculate the integral of this equation using partial fractions, which yields to

$$\begin{aligned}\int_1^{\exp(d_j\tau)} \frac{1-x}{x(1-g_j x)}dx &= \int_1^{\exp(d_j\tau)}\left[\frac{1}{x} - \frac{1-g_j}{1-g_j x}\right]dx \\ &= \left[lnx + \frac{1-g_j}{g_j}\ln(1-g_j x)\right]_{x=1}^{\exp(d_j\tau)} \\ &= \left[d_j\tau + \frac{1-g_j}{g_j}ln\left(\frac{1-g_j e^{d_j\tau}}{1-g_j}\right)\right].\end{aligned} \tag{4.61}$$

Inserting the integral and the values for d_j, Q_j and g_j again yields to

$$\mathbf{C_j(\tau,\phi) = ri\phi\tau + \frac{a}{\sigma^2}\left[(b_j - \sigma\rho i\phi + d_j)\tau - 2\ln\left(\frac{1-g_j e^{d_j\tau}}{1-g_j}\right)\right]} \tag{4.62}$$

as a solution for C_j, where $a = \kappa\theta$. Since we used the initial conditions the constant K_1 equals zero (Rouah, 2013). Having solutions for D_j and C_j as part of the characteristic function (4.49), the initial derivation of the Heston model is concluded.

4.2. Problems and extensions of the Heston Model

4.2.1. Problems with the integrant

So far, we derived and explained the Heston Model. Unfortunately, there are some problems with the basic version of the model, found by Kahl and Jäckel (2005) and Albrecher et al (2007). These result in inaccuracies in the numerical integration, which we want to avoid, since the integrand plays a major role in the Heston Model. We know that the behavior of the integrand depends on the values of the

parameters. For some values, the integrand is well-behaved, and the numerical integration works properly. For other values, the integrand is not well-behaved, which can cause a problem for the numerical integration. Therefore, we need to identify the issues and solve them to gain optimal results for the overall numerical valuation of the model.

The first occurring problem is that the integrand is not defined at $\phi=0$, even if the area of integration is [0,∞). Consequently, the integration has to start at a very small number close to zero. Because we are not starting at the original starting point, it is important that the integrand must not be too steep at the point to avoid inaccuracies in the calculation.

The second known problem is that the integrand might contain discontinuities. To illustrate this issue, we closely follow Ruoah (2013) with his example. He used two sets of integrands in the range of $\phi \in (0,10]$, whereas we only use one integrand, but therefore are plotting a surface, using τ as another variable. With $\kappa = 10$, $\theta = 0.05$, $v_0 = 0.05$, $\rho = -0.9$, $r = 0$, $S_0 = 90$ and $K = 90$ and $\sigma = 0{,}75$, we can observe the result in figure 4.1. The integrand shows great discontinuities for several ϕ and τ combinations, without any logical, financial valuation reason. Only somewhen after an integration range of $\phi \approx 10$ the integrand becomes constant for all shown maturities.

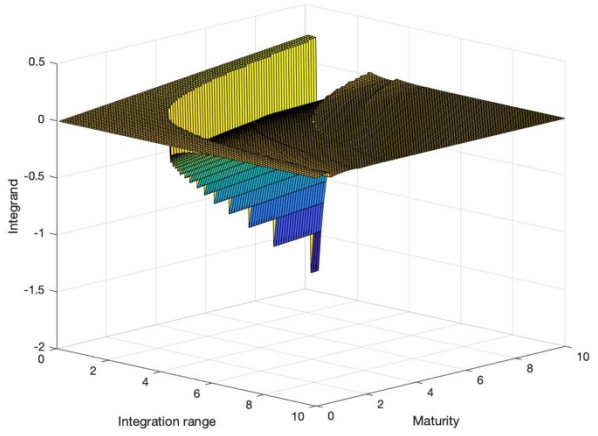

Figure 4.1: Discontinuities of the integrand, own representation

The third and last problem is a possible oscillation of the integrand. Again, following Ruoah (2013) and his example closely, we are plotting a surface with τ as another variable. We use $\kappa = 10$, $\theta = 0.01$, $v_0 = 0.01$, $\rho = -0.9$, $r = 0$, $S_0 = 7$ and $K = 10$ *and* $\sigma = 0{,}175$ for the parameters. Only way beyond $\phi \approx 100$, the integrand becomes flat. Another issue we can observe here is that the integrands are very steep at the beginning, meaning we need a very fine grid to avoid inaccuracies, as explained before.

Discontinuities are observable as well. To sum up, these issues affect the quality of the basic Heston Model. Fortunately, Albrecher et al (2007) discovered a simple solution for most of these problems.

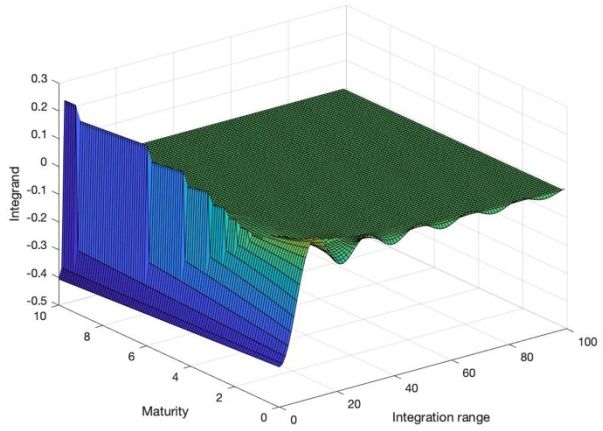

Figure 4.2: Oscillation of the integrand, own representation

4.2.2. The Little Heston Trap

When Albrecher et al (2007) published their paper, there were already two different formulations of the Heston Model in the academic literature available. The first one is the basic model that was subject to the derivation in this thesis. The other one is formulated slightly different, but in the end, they are the same. The advantage of the second formulation is that the second one leads to a characteristic function which is better behaved and, therefore, more applicable for numerical integration. Implementing the new formulation only requires two minor changes.

Firstly, we multiply D_j (4.58) with $exp(-d_j\tau)$ in the numerator and denominator, which leads to the same form but slightly different structure, namely

$$\boldsymbol{D_j(\tau,\phi) = \frac{b_j - \sigma\rho i\phi - d_j}{\sigma^2}\left(\frac{1 - e^{-d_j\tau}}{1 - c_j e^{-d_j\tau}}\right)} \tag{4.63}$$

where

$$\boldsymbol{c_j = \frac{1}{g_j} = \frac{b_j - \sigma\rho i\phi - d_j}{b_j - \sigma\rho i\phi + d_j}.}$$

Secondly, we are deriving C_j, as we did before by integration, which leads to

$$\boldsymbol{C_j(\tau,\phi) = ri\phi\tau + \frac{\kappa\theta}{\sigma^2}\left[(b_j - \sigma\rho i\phi + d_j)\tau - 2ln\left(\frac{1 - c_j e^{-d_j\tau}}{1 - c_j}\right)\right]}. \tag{4.64}$$

We can now substitute equation (4.63) with (4.58) and (4.64) with (4.62). The characteristic function (4.49) stays the same. Plotting the integrand

$$\boldsymbol{Re\left[\frac{e^{-i\phi lnK} f_j(\phi; x, v)}{i\phi}\right]} \tag{4.65}$$

from equation (4.38) for the two different formulations for the characteristic function f_1 with $\kappa = 1.5768$, $\theta = 0.0398$, $v_0 = 0.0175$, $\rho = -0.5711$, $r = 0$, $S_0 = 100$ and $K = 100$ and $\sigma = 0.5751$ as Albrecher et al (2007) did, shows us the difference in figure 4.3. The time to maturity is flexible again. While the original Heston formulation from Heston (1993) shows major discontinuities, the new formulation from Albrecher at al. (2007) is smooth. The trap is the area between the two surfaces.

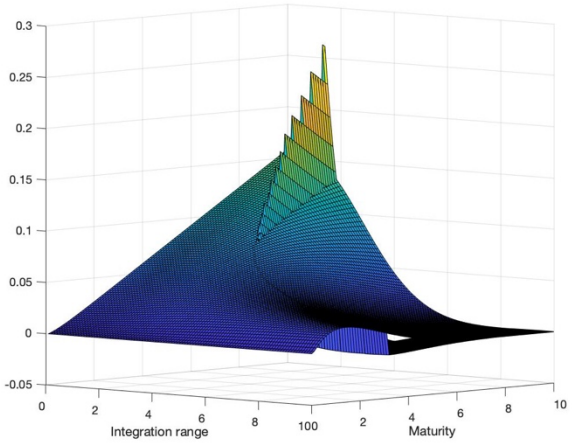

Figure 4.3: The little Heston Trap, own representation

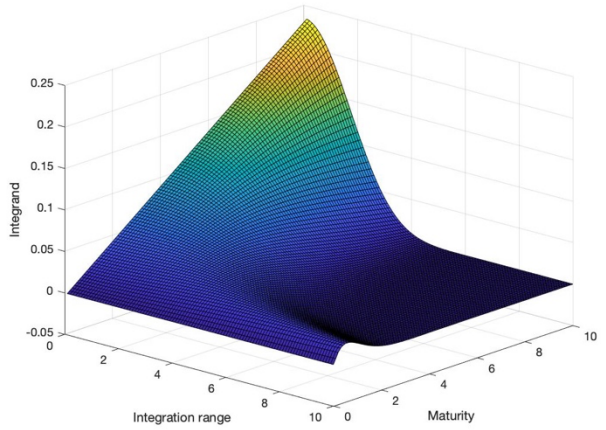

Figure 4.4: Integrand with the Albrecher et al. (2007) formulation, own representation

The discontinuities from figure 4.1 are eliminated as well (Figure 4.4), while the oscillation is still observable (Figure 4.5). The new formulation was not able to eliminate it. Also, the integrand is still very steep close to $\phi = 0$, as we also already described before.

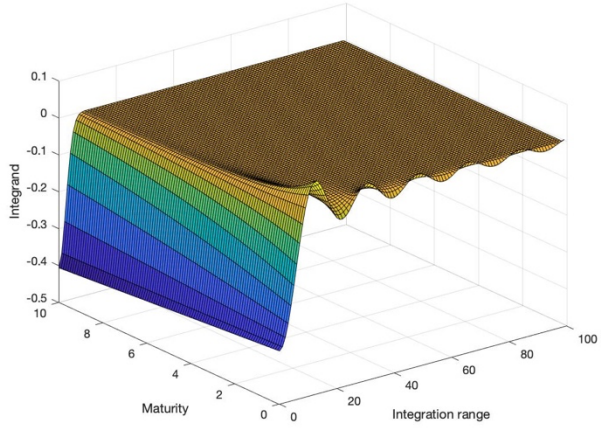

Figure 4.5: Oscillation with the Albrecher at al. (2007) formulation, own representation

Kahl and Jäckel (2005) as well as Zhu (2010) found different algorithms to overcome the same issue as the Albrecher et al. (2007) solution does. Anyway, since the Little Heston Trap was discovered, these solutions are obsolete.

4.2.3. Consolidation of the integrals and Characteristic Functions

Besides the processed problems with the integrand, there is another major hurdle the original Heston formulation needs to take, which is the calculation of the two integrands for P_1 and P_2. When calibrating the model, the two integrals need to be calculated many times, resulting in the need of a huge computational power and lots of computation time. Lewis (2000) and Attari (2004) both found a problem for that solution. The key is to eliminate one of the integrals, so that only one numerical integration is subject to the overall calculation, reducing computation time by almost one half. The results are the same. By inserting the formulars for the probabilities P_1 and P_2 into the formular for the call price

$$\boldsymbol{C(K) = S_t e^{-q\tau} P_1 - K e^{-r\tau} P_2} \tag{4.66}$$

and rearranging the terms, we receive

$$\begin{aligned} \boldsymbol{C(K)} &= \boldsymbol{\frac{1}{2} S_t e^{-q\tau} - \frac{1}{2} K e^{-r\tau}} \\ &+ \boldsymbol{\frac{1}{\pi} \int_0^{\infty} Re\left[\frac{e^{-i\phi lnK}}{i\phi} \left(S_t e^{-q\tau} f_1(\phi; x, v) - K e^{-r\tau} f_2(\phi; x, v) \right) \right] d\phi} \end{aligned} \tag{4.67}$$

for the call price. To calculate the according put price, we simply can use the put-call-parity as usual.

4.3. American Options in the Heston Model

The introduced basic version of the Heston Model and its extensions are not able to calculate values for American options. To value them, numerical methods are used, such as the Monte Carlo simulation based on the idea of Longstaff and Schwartz (2001) or the finite difference application by Brennan and Schwartz (1978). These methods can also be used to calculate American option values in the Heston Model. We decided to present the Explicit Finite Difference Method (FDE) in the Heston Model to value American put options in the numerical part of this work.

To implement the FDE in the Heston Model, the first step is to figure a way out to solve the Heston PDE 4.19 with $\lambda = 0$. To do so, the FDE uses a discrete grid for the price ($i = 0, \dots, N_S$), the volatility ($j = 0, \dots, N_V$) and the maturity ($n = 0, \cdots, N_T$). The value of a derivative in the FDE for a European call at the maturity *n+1* is defined as

$$U_{i,j}^{n+1} = U_{i,j}^{n} + dt[\frac{1}{2}v_j S_i^2 \frac{\partial^2}{\partial S^2} + \frac{1}{2}\sigma^2 v_j \frac{\partial^2}{\partial v^2} + \sigma\rho v_j S_i \frac{\partial^2}{\partial v \partial S} + (r-q)S_i \frac{\partial}{\partial S} + \kappa(\theta - v_j)\frac{\partial}{\partial v} - r]U_{i,j}^{n}. \quad (4.68)$$

To evaluate $U_{i,j}^{n+1}$, the derivations need to be replaced by finite difference approximations. These are simple for a uniform grid and a little more complex for a non-uniform grid. However, we will proceed with a non-uniform grid, since the results promise to be more accurate, even if fewer grid points are needed (Ruoah, 2013). The limits of the grid are set by the minimum and maximum values for *S, v* and *t,* denoted by $S_{min}=0$, $v_{min}=0$ and $t_{min}=0$ and S_{max}, v_{max} and $t_{max}=\tau$, respectively.

The discrete grid consists of nods which are either interior or on the boundary. To calculate the derivate value at each nod, we need the central difference approximation for the derivatives in 4.68. For the first order of interior nods these are

$$\frac{\partial U}{\partial S}(S_i, v_j) = \frac{U_{i+1,j}^{n} - U_{i-1,j}^{n}}{S_{i+1} - S_{i-1}} \quad (4.69)$$

and

$$\frac{\partial U}{\partial S}(S_i, v_j) = \frac{U_{i,j+1}^{n} - U_{i,j-1}^{n}}{v_{j+1} - v_{j-1}}. \quad (4.70)$$

For the second order they are

$$\frac{\partial^2 U}{\partial S^2}(S_i, v_j) = \frac{U_{i-1,j}^{n}}{(S_i - S_{i-1})(S_{i+1} - S_{i-1})} - \frac{2U_{i,j}^{n}}{(S_i - S_{i-1})(S_{i+1} - S_i)} + \frac{U_{i+1,j}^{n}}{(S_{i+1} - S_i)(S_{i+1} - S_{i-1})} \quad (4.71)$$

and

$$\frac{\partial^2 U}{\partial v^2}(S_i, v_j) = \frac{U^n_{i,j-1}}{(v_j - v_{j-1})(v_{j+1} - v_{j-1})} - \frac{2U^n_{i,j}}{(v_j - v_{j-1})(v_{j+1} - v_j)} + \frac{U^n_{i,j+1}}{(v_{j+1} - v_j)(v_{j+1} - v_{j-1})}. \tag{4.72}$$

Finally, for the mixed derivate the approximation is

$$\frac{\partial^2 U}{\partial S \partial v}(S_i, v_j) = \sum_{k,l} a_{k,l} U^n_{i+k,j+l} \tag{4.73}$$

for *k=l=[-1,0,1].* For a detailed list see Ruoah (2013). For the boundary nods values from outside of the grid are needed, which are approximated by either forward or backward differences. To finally roll out the finite difference scheme, boundary conditions need to be set for the PDE. These depend on the kind of option and are introduced by Heston (1993).

As a last step, the introduced approximations submit the derivatives in 4.68. Using a matrix to reflect the grid mathematically, values for all nods can be calculated. For the calculation in MatLab we also use an interpolation to reflect the correct current value of the underlying, which might not be possible otherwise, depending on the discretion of the grid. Note that for American options we need to implement the early exercise condition at every nod with

$$U^{n+1}_{i,j} = \max\left(K - S_i, U^{n+1}_{i,j}\right). \tag{4.74}$$

5. Parameter analysis

5.1. Effect of the Correlation Parameter

Since the Heston Model contains parameters, that we do not use in other models, we want to investigate them. By doing so, we can expose some of the favorable characteristics of the Heston Model. Firstly, we want to have a closer look at ρ, which indicates the correlation between two Brownian motions. Moreover, it controls the skewness of the distribution of lnS_T. If the volatility increases and $\rho > 0$, the stock price will increase as well. If $\rho < 0$, the stock price would decrease and if $\rho = 0$, a change in the volatility would have no effect on the skewness of the distribution. Underlying this relationship, we replicate the plot of Ruoah (2013), who used the same settings at Heston (1993). The parameters are set to $\kappa = 2$; $\theta = 0{,}01$; $v_t = 0{,}01; \sigma = 0{,}1$; $\tau = 0{,}5; r = 0$ and *K = 100.* The density of lnS_T can be obtained by inverting the characteristic function $f_2(\phi)$ and applying a numerical integration scheme.

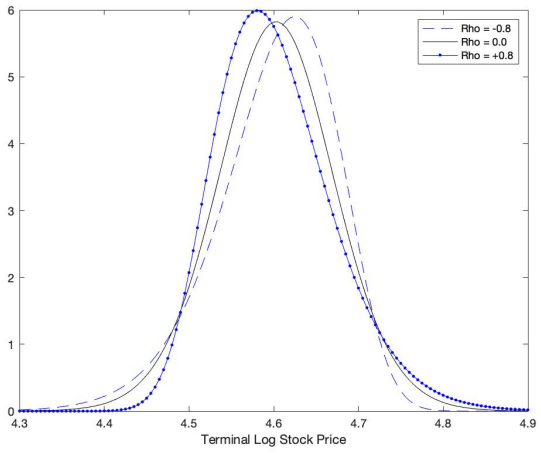

Figure 5.1: Relationship between skewness and correlation, own representation

We can observe that there is a relationship between skewness and correlation. As Heston (1993) explains, a negative correlation implies a rise in the variance and a decrease in the stock price. That leads to fattening the left tail and thinning the right tail of the distribution (blue dashed). If the correlation is positive, it will have the opposite effect (blue dotted). Our plot confirms this relationship. As financial data tends to be negatively skewed instead of being 0-skewed, this parameter has the potential to improve the accurateness for option prices over models without this feature. We will review and verify this in the numerical part of this work.

5.2. Effect of the Volatility of the Variance Parameter

The volatility of the variance parameter, σ, has a useful characteristic as well. It controls the kurtosis, meaning the higher σ, the higher the dispersion of the variance process. Using the same data as in the prior example, except for $\rho = 0$ and a flexible σ. Figure 5.2 shows the positive correlation between σ and the kurtosis, having a higher σ concludes in a higher kurtosis and fatter tails compared to smaller values of σ. Therefore, this parameter also has the potential to improve the accurateness for option prices over models without this feature. Again, we will review and verify this in the numerical part of this work.

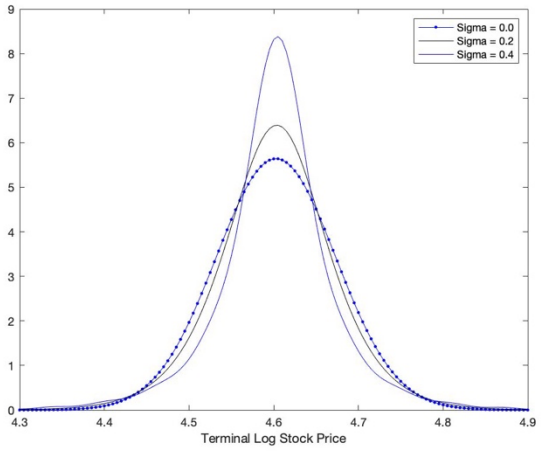

Figure 5.2: Relationship between kurtosis and volatility of the variance, own representation

5.3. Comparison with the Black Scholes-Merton Model

The parameter analysis becomes more interesting and valuable when compared to the basic model, the Black Scholes Model. The sensible impact of ρ and σ on the stock price already gave us a hint, that the option prices generated by the Heston Model should differ from the ones generated by the Black-Scholes-Merton Model. Heston (1993) shows that the difference between Heston and Black Scholes prices depends on the moneyness of the stock price. To show this, we use the parameters from Table 1 from (Heston 1993), subtract the Black Scholes prices from the Heston prices and plot the result. The strike price K = 90 and we use one negative and one positive correlation value. In order to compare the methods accurately, the BSM volatilities need to be matched to the Heston price. For the implementation, the BSM volatility has to be defined as the standard deviation of the distribution of the returns lnS_T/S_0. It can be clearly seen that in the case of positive correlation OTM calls are more expensive generated by the Heston Model than those of the BSM Model.

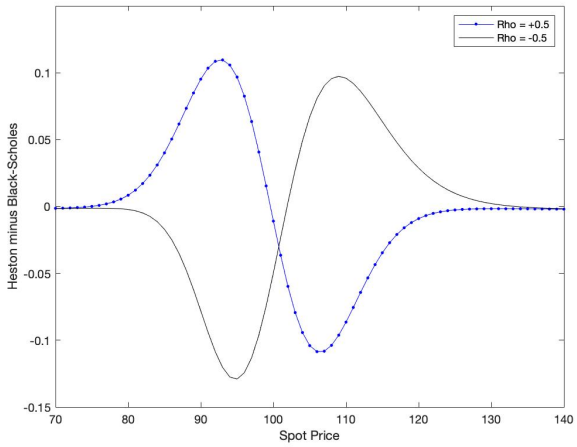

Figure 5.3: Comparison with BSM for different correlations, own representation

To explain this difference, we need to have a look at Figure 5.1 again. Having $\rho > 0$, the skew in the distribution of lnS_T is positive. Thus, the right side of the distribution has more weight due to the fat right tail, and therefore Heston OTM calls (left side of figure 5.3) are more expensive than BSM OTM calls, where there is the same weight assigned to both sides. The opposite is the case for ITM call options (right side of figure 5.3.). As we can observe, in case of $\rho < 0$, the relationships are the other way around.

We can extend the comparison between Heston and Black Scholes prices by having a look at the difference occurring when using different values for σ. All data is set as before, but $\rho = 0$ and σ is now variable. The result is displayed in Figure 5.4.

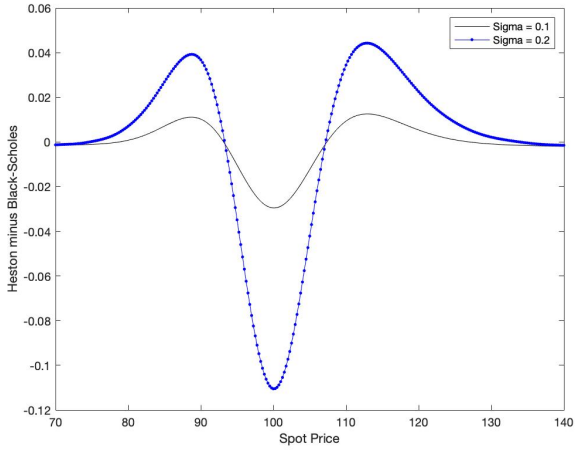

Figure 5.4: Comparison with BSM for different volatilities of the variance, own representation

We can observe that the Heston price is higher for ITM and OTM calls, but lower for ATM calls. This is the logic consequence from the thicker tails we saw in Figure 5.2. More weight is assigned to the tails, and therefore to Spot prices *S*, that make the call option be ITM or OTM. Also, the higher σ, the greater is the difference between Heston and Black Scholes prices.

6. Numerical analysis

6.1. General conditions and CPU

The aim of the numerical analysis is to evaluate in practical terms what has been introduced so far in this work regarding the Heston Model. We run the overall process, from the access of the needed input data over to the calibration to the final calculation of Heston Model option values. These values are then evaluated using real market data, BSM- and CRR-values as a comparison. We test European call option on the S&P500 with the basic Heston Model and American put options on Apple with the Heston FDE Model. All calculations were done using MatLab Version R2022a Update 1 (9.12.0.1927505) and the scripts from Rouah (2013) on a MacBookPro14.1 with an IntelCore i5 with 2.3GHz and 8GB memory.

6.2. Data

All desired input data was downloaded on the 16th February 2022 from the Thomson Reuters database Refinitiv Eikon. For the European S&P options, we downloaded end of day data, value 03.08.2021 for four maturities (45, 73, 108 and 136 days) and 29 strike prices (4160 to 4720 in steps of 20). Next to the maturities and strikes, we also downloaded the option price, the spot price of the underlying (4423.16) and the interest rate for 3-months treasury bills (0.05%). Using all given data and the BSM Model, we retrieved the implied volatility of every single option with the goal seek function in Excel. The results in table 6.1 already give a glance at the changing volatility and possible problems trying to reflect these values with one single value as it is done in the BSM Model. We also downloaded the data with the exact same characteristics with value 04.08.2021 to have benchmark values for our final comparison. Obviously, all maturities are -1 day and the value of the S&P500 changed to 4402.65 points.

The same was repeated for the American put options on Apple. We downloaded end of day data with value 03.08.2021 for four maturities (45, 73, 108 and 136 days) and eight strike prices (135 to 170 in steps of 5). The range of available options was smaller than for the S&P500. The spot price was 147.36 and the risk-free interest rate was 0.05% again. Here the implied volatility was retrieved using the data and the CRR Model with increments of *dt=0.0001*, since the BSM Model only works for European options. The calculations were done in MatLab and the results are summed up in table 6.1 as well.

Option values	Maturity			
Strike	45	73	108	136
4720	1,95	9,20	22,60	35,50
4700	2,57	11,15	26,25	40,30
4680	3,40	13,45	30,45	45,60
4660	4,20	16,30	35,25	51,50
4640	5,60	19,70	40,65	57,90
4620	7,45	23,80	46,70	64,95
4600	9,85	28,60	53,45	72,55
4580	13,15	34,20	60,85	80,75
4560	17,10	40,75	68,95	89,55
4540	22,30	48,10	77,70	98,90
4520	28,60	56,40	87,15	108,85
4500	36,30	65,70	97,25	119,25
4480	44,95	75,60	107,90	130,15
4460	54,95	86,55	119,25	141,55
4440	66,15	98,20	131,00	153,40
4420	78,30	110,55	143,40	165,65
4400	91,30	123,55	156,25	178,40
4380	105,20	137,10	169,50	191,50
4360	119,70	151,15	183,10	204,90
4340	134,75	165,60	197,10	218,60
4320	150,30	180,45	211,45	232,60
4300	166,15	195,70	226,10	246,90
4280	182,60	211,30	241,05	261,50
4260	199,15	227,10	256,15	276,35
4240	216,00	243,15	271,55	291,20
4220	233,05	259,45	287,25	306,50
4200	250,25	275,95	303,15	322,00
4180	267,75	292,65	319,25	337,60
4160	285,35	309,45	335,45	353,50

Implied volatilities	Maturity			
Strike	45	73	108	136
4720	0,0993	0,1081	0,1157	0,1212
4700	0,0988	0,1083	0,1166	0,1225
4680	0,0985	0,1086	0,1178	0,1239
4660	0,0968	0,1093	0,1192	0,1255
4640	0,0969	0,1102	0,1208	0,1271
4620	0,0973	0,1114	0,1225	0,1290
4600	0,0979	0,1129	0,1245	0,1309
4580	0,0993	0,1146	0,1265	0,1329
4560	0,1006	0,1168	0,1288	0,1351
4540	0,1028	0,1191	0,1311	0,1373
4520	0,1053	0,1217	0,1336	0,1397
4500	0,1085	0,1247	0,1362	0,1421
4480	0,1116	0,1276	0,1389	0,1445
4460	0,1153	0,1309	0,1417	0,1470
4440	0,1194	0,1343	0,1445	0,1495
4420	0,1236	0,1379	0,1475	0,1521
4400	0,1279	0,1415	0,1505	0,1547
4380	0,1325	0,1452	0,1535	0,1574
4360	0,1369	0,1489	0,1564	0,1600
4340	0,1413	0,1525	0,1594	0,1626
4320	0,1457	0,1561	0,1624	0,1652
4300	0,1498	0,1597	0,1654	0,1678
4280	0,1542	0,1634	0,1684	0,1704
4260	0,1581	0,1668	0,1712	0,1730
4240	0,1619	0,1702	0,1740	0,1754
4220	0,1655	0,1735	0,1769	0,1779
4200	0,1687	0,1768	0,1798	0,1805
4180	0,1720	0,1799	0,1826	0,1829
4160	0,1749	0,1828	0,1853	0,1854

Option values	Maturity			
Strike	45	73	108	136
170	23,08	23,50	24,53	25,08
165	18,25	18,90	20,23	20,95
160	13,68	14,60	16,28	17,15
155	9,50	10,80	12,73	13,70
150	6,06	7,56	9,62	10,70
145	3,55	5,10	7,15	8,20
140	2,04	3,35	5,22	6,15
135	1,19	2,23	3,80	4,59

Implied volatilities	Maturity			
Strike	45	73	108	136
170	0,2753	0,2520	0,2651	0,2592
165	0,2505	0,2410	0,2621	0,2576
160	0,2365	0,2335	0,2571	0,2565
155	0,2264	0,2325	0,2566	0,2520
150	0,2240	0,2322	0,2550	0,2507
145	0,2290	0,2385	0,2627	0,2603
140	0,2438	0,2486	0,2710	0,2695
135	0,2660	0,2695	0,2828	0,2740

Table 6.1: Option values and implied volatilities for the S&P500 and Apple stock

6.3. Calibration of the model

One important step in the application of the Heston Model is its calibration. Economic models like the Heston Model require a set of input data or parameters, which can be observed in the market, received from experts or literature. The Heston Model is an exception here. The needed inputs are not available, since the model works with own parameters, that are not directly observable in the market. The idea here is to estimate these parameters based on other historical parameters observable in the market, like the strike price, underlying price, interest rates, etc. The accurate estimation is crucial to the Heston Model, because the model would fail using badly estimated values, making all theoretical underlying work worthless (Jacquier & Jarrow, 2000). Therefore, a calibration of the model parameters is used. A calibration in this sense is a process in which the desired parameters are calculated based on known data using an algorithm. For the Heston Model, this algorithm in most cases is a loss function (Mikhailov & Nögel (2004) and Rouah (2013)) minimizing an error.

We tested four different objective function and then chose the most accurate one. The most popular one is the mean error sum of squares (MSE) loss function, which minimizes

$$\frac{1}{N}\sum_{t,k} w_{tk}(C_{tk} - C_{tk}^{\Theta})^2 \tag{6.1}$$

with respect to Θ. The relative mean error sum of squares (RMSE) minimizes

$$\frac{1}{N}\sum_{t,k} w_{tk}\,\frac{(C_{tk} - C_{tk}^{\Theta})^2}{C_{tk}}. \tag{6.2}$$

Using implied volatilities instead of option prices, the implied volatility mean error sum of squares (IVMSE) minimizes

$$\frac{1}{N}\sum_{t,k} w_{tk}(IV_{tk} - IV_{tk}^{\Theta})^2. \tag{6.3}$$

The fourth and last objective function is the one introduced by Christoffersen et al. (2009) (CHJ), which is

$$\frac{1}{N}\sum_{t,k} w_{tk}\,\frac{(C_{tk} - C_{tk}^{\Theta})^2}{BSVega_{tk}^2}, \tag{6.4}$$

where

$$BSVega_{tk} = Se^{(-q\tau)}n(d_{tk})\sqrt{\tau_k}$$

with

$$d_{tk} = \frac{\log\left(\frac{S}{K_k}\right) + (r - q + \frac{IV_{tk}^2}{2})\,\tau_t}{IV_{tk}\sqrt{\tau_k}}.$$

BSVega represents the Black-Scholes sensitivity of the option price regarding the implied volatility. For our work it is from great importance to use the most accurate estimation of the parameters. Further analyses are not the objective of this work and are therefore not proceeded. For more detailed information about the objective function refer to Ruoah (2013), Christoffersen & Jacobs (2004) or Mikhailov & Nögel (2003).

The results of our calibration are summerized in table 6.2 for the European call options on the S&P500 and in table 6.3 for the American put options on Apple. The starting values are taken from Guillaume and Schoutens (2012), except kappa, where we were able to calculate better results with a value of 0.4.

	kappa	theta	sigma	v0	rho	IVMSE	time
initial values	0,4	0,0551	0,1927	0,0746	-1		
MSE	7,3711	0,0453	1,5371	0,0114	-0,731	5,34E-06	8,40
RMSE	7,9674	0,0422	1,452	0,0113	-0,737	5,05E-06	12,84
IVMSE	0,5982	0,2968	1,6649	0,0159	-0,6069	5,56E-05	48,34
CHJ	6,6143	0,046	1,3369	0,0106	-0,7384	4,19E-06	15,83

Table 6.2: Calibrated parameters for the S&P500 options, whole sample

In both cases the CHJ objective function seems to deliver the best results, based on the IVMSE value. It is important to note that in all cases we used the Gauss Laguerre quadrature with 32 points to obtain the option prices. Working with only 16 points or using the Gauss Lobatto quadrature did not deliver more accurate results. Since there is no consensus on which method might be the best to use (Ruoah 2013), we rely on the found results and proceed with the calibrated parameters.

	kappa	theta	sigma	v0	rho	IVMSE	time
initial values	0,4	0,0551	0,1927	0,0746	-1		
MSE	3,7388	0,0958	3,0831	0,0355	-0,2026	2,88E-05	6,60
RMSE	11,6159	0,0981	2,8038	0,0396	-0,2081	2,90E-05	3,90
IVMSE	0,6794	0,3648	0,5559	0,0408	-0,0822	1,66E-04	2,08
CHJ	12,1733	0,0976	2,8886	0,0378	-0,1994	2,86E-05	5,10

Table 6.3: Calibrated parameters for the Apple options

6.4. Results for European call options

In this step we present the numerical results and compare the Heston Model prices to real markets prices and BSM prices for European call options on the S&P500, value 04.08.2021. The real market data is already downloaded. To calculate the BSM prices, we first need to find the single volatility that minimizes the relative mean absolute error (RMAE)

$$\frac{1}{N}\sum_{t,k}\frac{\left|C_{tk}-C_{tk}^{\Theta}\right|}{C_{tk}} \tag{6.5}$$

of the BSM prices to the real market prices, value 03.08.2021. For our data, the calibrated volatility is 11.29%. Using this value to calculate all desired BSM prices value 04.08.2021, we receive the results in table 6.4. The market values are shown as well. The differences are obvious, which is reflected in a RMAE of 23.24%.

Market Option Prices 04.08.21				
	44	72	107	135
4720	1,38	7,50	19,70	31,85
4700	1,81	9,20	23,00	36,08
4680	2,30	11,15	26,75	41,20
4660	3,08	13,60	31,10	46,70
4640	4,05	16,55	36,05	52,75
4620	5,45	20,10	41,65	59,40
4600	7,40	24,35	47,90	66,65
4580	9,80	29,40	54,85	74,45
4560	13,10	35,30	62,50	82,90
4540	17,45	42,05	70,85	91,90
4520	22,90	49,75	79,90	101,50
4500	29,40	58,35	89,60	111,55
4480	37,65	67,85	99,95	122,15
4460	46,90	78,25	110,90	133,25
4440	57,40	89,40	122,40	144,90
4420	69,00	101,40	134,45	156,90
4400	81,55	114,25	147,00	169,40
4380	94,95	127,20	160,00	182,25
4360	109,10	141,10	173,25	195,35
4340	123,85	155,30	187,05	208,85
4320	139,10	169,90	201,10	222,70
4300	154,80	184,90	215,55	236,75
4280	170,85	200,25	230,40	251,20
4260	187,05	215,95	245,35	265,90
4240	203,75	231,85	260,75	280,75
4220	220,60	247,90	276,25	295,90
4200	237,75	264,10	291,95	311,25
4180	255,05	280,60	307,85	326,75
4160	272,60	297,30	323,95	342,45

Black Scholes Option Prices 04.08.21				
	44	72	107	135
4720	2,72	8,63	17,76	25,50
4700	3,54	10,34	20,34	28,60
4680	4,57	12,33	23,22	32,00
4660	5,85	14,63	26,42	35,74
4640	7,42	17,29	29,99	39,81
4620	9,35	20,33	33,93	44,26
4600	11,68	23,80	38,27	49,08
4580	14,48	27,73	43,05	54,31
4560	17,80	32,16	48,28	59,96
4540	21,71	37,12	53,99	66,05
4520	26,27	42,66	60,20	72,60
4500	31,54	48,81	66,92	79,62
4480	37,58	55,59	74,19	87,13
4460	44,43	63,04	82,01	95,13
4440	52,14	71,17	90,40	103,64
4420	60,75	80,00	99,37	112,67
4400	70,26	89,55	108,92	122,22
4380	80,70	99,82	119,07	132,30
4360	92,07	110,82	129,82	142,91
4340	104,34	122,53	141,16	154,05
4320	117,49	134,96	153,08	165,72
4300	131,49	148,07	165,59	177,91
4280	146,29	161,86	178,67	190,61
4260	161,83	176,28	192,30	203,82
4240	178,05	191,32	206,47	217,52
4220	194,89	206,94	221,15	231,71
4200	212,28	223,09	236,34	246,35
4180	230,14	239,74	251,99	261,44
4160	248,42	256,84	268,09	276,96

Table 6.4: Option prices for the S&P500 from the market and with the BSM Method

The results of the Heston Method are presented in table 6.5. The percentage error to the real markets values for every single value is shown as well. For a more friendly presentation, we also used a heat map, making patterns in the values visible. The overall RMAE is 6.40%. Therefore, we can conclude that the Heston Model performs better than the BSM Model for our data. From the heatmap in table 6.5 we can conclude two more things: long term options are way more accurate reflected than short term options and ITM options are why more accurate reflected than OTM options. Regarding the previous parameter analysis, we can confirm the made statements. The negatively skewed distribution of *ln(S)* due to the negative ρ represents financial data better than a normal distribution offered by the BSM Model, and therefore is able to produce more accurate results (see figure 5.1). The highly positive σ suggests a

leptokurtic distribution, which is favorable as well (see figure 5.2). To value the statements regarding the comparison between the Heston and BSM Model, we introduce table 6.6. The results clearly confirm the results from the parameter analysis, specially from figures 5.3 and 5.4. Due to the negative ρ and following fat left tail, ITM call options are priced higher in the Heston than in the BSM Model. OTM calls on the other hand are priced lower, at least for short maturities.

Heston prices 04.08.21 whole sample CHJ				
	44	72	107	135
4720	1,56	6,87	18,39	31,64
4700	2,51	8,30	21,21	35,72
4680	3,44	9,93	24,47	40,31
4660	4,33	11,84	28,26	45,46
4640	5,21	14,14	32,64	51,21
4620	6,21	16,97	37,71	57,59
4600	7,52	20,49	43,50	64,61
4580	9,35	24,82	50,05	72,26
4560	11,99	30,11	57,40	80,55
4540	15,68	36,43	65,51	89,43
4520	20,65	43,82	74,38	98,99
4500	27,05	52,28	83,94	108,91
4480	34,95	61,74	94,15	119,42
4460	44,28	72,12	104,96	130,42
4440	54,95	83,30	116,30	141,88
4420	66,74	95,15	128,12	153,76
4400	79,43	107,55	140,41	166,06
4380	92,79	120,43	153,13	178,76
4360	106,62	133,73	166,72	191,85
4340	120,78	147,43	179,83	205,30
4320	135,22	161,53	193,79	219,09
4300	149,95	176,06	208,14	233,21
4280	165,05	191,05	222,86	247,62
4260	180,62	206,50	237,91	262,30
4240	196,74	222,41	253,26	277,21
4220	213,47	238,72	268,86	292,34
4200	230,80	255,37	284,67	307,66
4180	248,66	272,28	300,65	323,17
4160	266,91	289,35	316,78	338,85

Heston prices 04.08.21 whole sample CHJ % errors				
	44	72	107	135
4720	13,5%	8,4%	6,6%	0,7%
4700	38,7%	9,8%	7,8%	1,0%
4680	49,6%	10,9%	8,5%	2,2%
4660	40,8%	12,9%	9,1%	2,7%
4640	28,6%	14,6%	9,5%	2,9%
4620	13,9%	15,6%	9,5%	3,0%
4600	1,6%	15,9%	9,2%	3,1%
4580	4,6%	15,6%	8,8%	2,9%
4560	8,5%	14,7%	8,2%	2,8%
4540	10,1%	13,4%	7,5%	2,7%
4520	9,8%	11,9%	6,9%	2,5%
4500	8,0%	10,4%	6,3%	2,4%
4480	7,2%	9,0%	5,8%	2,2%
4460	5,6%	7,8%	5,4%	2,1%
4440	4,3%	6,8%	5,0%	2,1%
4420	3,3%	6,2%	4,7%	2,0%
4400	2,6%	5,9%	4,5%	2,0%
4380	2,3%	5,3%	4,3%	1,9%
4360	2,3%	5,2%	3,8%	1,8%
4340	2,5%	5,1%	3,9%	1,7%
4320	2,8%	4,9%	3,6%	1,6%
4300	3,1%	4,8%	3,4%	1,5%
4280	3,4%	4,6%	3,3%	1,4%
4260	3,4%	4,4%	3,0%	1,4%
4240	3,4%	4,1%	2,9%	1,3%
4220	3,2%	3,7%	2,7%	1,2%
4200	2,9%	3,3%	2,5%	1,2%
4180	2,5%	3,0%	2,3%	1,1%
4160	2,1%	2,7%	2,2%	1,1%

Table 6.5: Option prices for the S&P 500 with the Heston Model and its errors, whole sample

It is interesting to note that the effect is not as symmetric as it is in the parameter analysis. This is due to the overlaying effect we have, caused by the high sigma. If we have a closer look, we can observe that the values for the 44 days-maturity reflect a combination of figures 5.3 and 5.4. Therefore, our data can confirm all the sensitivities we previously introduced in the parameter analysis.

In a next step, we want to test whether we are able to improve the quality of the Heston Model by splitting up our in-sample-data, value 03.08.21, into ITM, ATM and OTM samples. To do so, we divide the data with respect to the strike price. The first part is from 4160 to 4340 (ITM, 40 option values), the second from 4360 to 4520 (ATM, 36 option values) and the third from 4540 to 4720 (OTM, 40 option values). Each of

the calibrations delivered the best results using the RMSE objective functions. The parameter settings are shown in table 6.7. Note that the values for IVMSE are lower than the ones obtained for the whole sample calibration. Nevertheless, the results we receive applying the parameters to the Heston Model are worse than for the whole calibration. The RMAE worsened from 6.40% to 13.04%. Having a look at table 6.8, we can get from the heatmap that only for ITM options we have values that can compete with the ones from the whole sample calculation. The RMAE is 2.7% here compared to 2.8% before. Specially OTM options are inaccurate presented, with very high discrepancies for short maturities.

Heston minus BS values				
	44	72	107	135
4720	-1,16	-1,76	0,63	6,14
4700	-1,03	-2,04	0,87	7,12
4680	-1,13	-2,40	1,25	8,31
4660	-1,52	-2,79	1,84	9,72
4640	-2,21	-3,15	2,65	11,40
4620	-3,14	-3,36	3,78	13,33
4600	-4,16	-3,31	5,23	15,53
4580	-5,13	-2,91	7,00	17,95
4560	-5,81	-2,05	9,12	20,59
4540	-6,03	-0,69	11,52	23,38
4520	-5,62	1,16	14,18	26,39
4500	-4,49	3,47	17,02	29,29
4480	-2,63	6,15	19,96	32,29
4460	-0,15	9,08	22,95	35,29
4440	2,81	12,13	25,90	38,24
4420	5,99	15,15	28,75	41,09
4400	9,17	18,00	31,49	43,84
4380	12,09	20,61	34,06	46,46
4360	14,55	22,91	36,90	48,94
4340	16,44	24,90	38,67	51,25
4320	17,73	26,57	40,71	53,37
4300	18,46	27,99	42,55	55,30
4280	18,76	29,19	44,19	57,01
4260	18,79	30,22	45,61	58,48
4240	18,69	31,09	46,79	59,69
4220	18,58	31,78	47,71	60,63
4200	18,52	32,28	48,33	61,31
4180	18,52	32,54	48,66	61,73
4160	18,49	32,51	48,69	61,89

Table 6.6: CHJ option prices minus the BSM option prices

For our data we can conclude that it does not pay off to split up the data. Note that the calibrated parameters in table 6.7 show the same structure as the ones by CHJ for the whole sample. The starting values are the same as in table 6.2 and 6.3. The negative ρ and the high σ again represent the financial data, the values in average are still more accurate than the ones by BSM presented in table 6.4 with a mentioned RMAE of 23.24%.

	objective function	kappa	theta	sigma	v0	rho	IVMSE	EstTime
ITM	RMSE	22,2498	0,0280	1,8502	0,0047	-0,6980	1,44E-06	5,39
ATM	RMSE	16,2514	0,0391	2,9076	0,0088	-0,6486	1,54E-06	4,61
OTM	RMSE	15,2465	0,0385	1,9030	0,0004	-0,8175	3,11E-06	3,60

Table 6.7: Calibrated parameters for the S&P500 options, split sample

Heston prices Split Sample RMSE				
	44	72	107	135
4720	6,56	7,21	18,03	30,69
4700	6,01	8,19	21,10	34,95
4680	5,40	9,52	24,66	39,66
4660	4,85	11,32	28,74	44,86
4640	4,53	13,66	33,39	50,54
4620	4,59	16,64	38,63	56,72
4600	5,22	20,34	44,49	63,41
4580	6,58	24,85	50,98	70,61
4560	8,85	30,22	58,11	78,31
4540	12,19	36,49	65,88	86,51
4520	21,10	46,24	76,96	99,43
4500	26,38	54,18	86,06	108,91
4480	33,22	63,16	95,81	118,61
4460	41,72	73,14	106,19	129,41
4440	51,87	84,01	117,16	140,39
4420	63,54	95,71	128,67	151,85
4400	76,51	108,90	140,70	163,75
4380	90,51	121,08	153,22	176,07
4360	105,22	134,57	166,20	188,81
4340	119,05	148,68	182,19	205,41
4320	133,74	162,94	196,00	218,78
4300	148,66	177,71	210,16	232,46
4280	163,93	192,97	224,62	246,42
4260	179,70	208,69	239,36	260,65
4240	196,11	224,78	254,36	275,16
4220	213,23	241,18	269,60	289,92
4200	231,04	257,80	285,07	304,94
4180	249,42	274,56	300,77	320,19
4160	268,18	291,42	316,71	335,68

Heston prices Split Sample RMSE % Errors				
	44	72	107	135
4720	377,1%	3,9%	8,5%	3,6%
4700	232,0%	11,0%	8,3%	3,1%
4680	134,8%	14,6%	7,8%	3,7%
4660	57,7%	16,8%	7,6%	3,9%
4640	11,9%	17,5%	7,4%	4,2%
4620	15,8%	17,2%	7,3%	4,5%
4600	29,5%	16,5%	7,1%	4,9%
4580	32,9%	15,5%	7,1%	5,2%
4560	32,4%	14,4%	7,0%	5,5%
4540	30,1%	13,2%	7,0%	5,9%
4520	7,9%	7,1%	3,7%	2,0%
4500	10,3%	7,1%	4,0%	2,4%
4480	11,8%	6,9%	4,1%	2,9%
4460	11,0%	6,5%	4,2%	2,9%
4440	9,6%	6,0%	4,3%	3,1%
4420	7,9%	5,6%	4,3%	3,2%
4400	6,2%	4,7%	4,3%	3,3%
4380	4,7%	4,8%	4,2%	3,4%
4360	3,6%	4,6%	4,1%	3,3%
4340	3,9%	4,3%	2,6%	1,6%
4320	3,9%	4,1%	2,5%	1,8%
4300	4,0%	3,9%	2,5%	1,8%
4280	4,1%	3,6%	2,5%	1,9%
4260	3,9%	3,4%	2,4%	2,0%
4240	3,7%	3,0%	2,5%	2,0%
4220	3,3%	2,7%	2,4%	2,0%
4200	2,8%	2,4%	2,4%	2,0%
4180	2,2%	2,2%	2,3%	2,0%
4160	1,6%	2,0%	2,2%	2,0%

Table 6.8: Option prices for the S&P 500 with the Heston Model and its errors, split sample

For our next test, the high sigma turns out to be an obstacle. Before we use the FDE on the American put option data, we want to use it to calculate options prices for the European call options on the S&P500. Unfortunately, the FDE does not work with a sigma as high as we have calibrated it with the CHJ from table 6.2. We need a sigma < 1. Therefore, we use the exact same start values as Guillaume and Schoutens (2012) did, switching our kappa of 0.4 back to its original value of 0.3369. The new calibrated values fit well for the FDE Method. In this case we also used the RMSE objective function since it delivered a lower IVMSE than CHJ.

	kappa	theta	sigma	v0	rho	IVMSE	EstTime
CHJ	0,3882	0,311	0,8	0,0138	-0,7495	6,34E-06	5.243

Table 6.9: Calibrated parameters for the S&P500 options, FDE adjusted

Applying the parameters and using a grid consisting of 200 points for S, 100 for V and 5000 for T, we receive the values and relating percentage errors in table 6.10. The overall RMAE is only 4.87%, meaning the FDE Method is able to outperform the analytical solution we found in table 6.5. The more accurate overall value is mainly resulting from the decent percentage errors of the short term OTM options. The values notably more accurate. The maximal errors we found is 15.6% compared to 49.6% for table 6.5.

Heston FDE prices whole sample RMSE				
	44	72	107	135
4720	1,32	6,75	18,94	32,20
4700	1,70	8,03	21,60	35,92
4680	2,54	10,20	25,45	40,99
4660	3,39	12,36	29,30	46,03
4640	4,42	14,79	33,45	51,36
4620	6,30	18,46	38,98	58,02
4600	8,18	22,12	44,52	64,69
4580	10,71	26,52	50,73	71,94
4560	14,46	32,29	58,21	80,31
4540	18,21	38,06	65,68	88,68
4520	23,58	45,28	74,32	98,00
4500	30,11	53,53	83,76	107,99
4480	36,63	61,79	93,21	117,98
4460	46,03	72,21	104,23	129,22
4440	55,79	82,90	115,43	140,61
4420	66,28	94,10	127,00	152,30
4400	78,83	106,75	139,60	164,84
4380	91,38	119,39	152,20	177,38
4360	105,22	132,99	165,55	190,56
4340	119,61	147,01	179,23	204,02
4320	134,23	161,23	193,07	217,63
4300	149,81	176,25	207,60	231,85
4280	165,40	191,28	222,13	246,07
4260	181,65	206,88	237,17	260,76
4240	198,13	222,70	252,40	275,62
4220	214,85	238,72	267,82	290,66
4200	232,02	255,16	283,62	306,05
4180	249,20	271,60	299,42	321,45
4160	266,91	288,55	315,69	337,30

Heston FDE prices whole sample RMSE % Errors				
	44	72	107	135
4720	4,0%	10,0%	3,9%	1,1%
4700	6,1%	12,7%	6,1%	0,4%
4680	10,4%	8,5%	4,9%	0,5%
4660	10,2%	9,1%	5,8%	1,4%
4640	9,1%	10,6%	7,2%	2,6%
4620	15,6%	8,2%	6,4%	2,3%
4600	10,5%	9,2%	7,1%	2,9%
4580	9,3%	9,8%	7,5%	3,4%
4560	10,4%	8,5%	6,9%	3,1%
4540	4,4%	9,5%	7,3%	3,5%
4520	3,0%	9,0%	7,0%	3,4%
4500	2,4%	8,3%	6,5%	3,2%
4480	2,7%	8,9%	6,7%	3,4%
4460	1,9%	7,7%	6,0%	3,0%
4440	2,8%	7,3%	5,7%	3,0%
4420	3,9%	7,2%	5,5%	2,9%
4400	3,3%	6,6%	5,0%	2,7%
4380	3,8%	6,1%	4,9%	2,7%
4360	3,6%	5,7%	4,4%	2,5%
4340	3,4%	5,3%	4,2%	2,3%
4320	3,5%	5,1%	4,0%	2,3%
4300	3,2%	4,7%	3,7%	2,1%
4280	3,2%	4,5%	3,6%	2,0%
4260	2,9%	4,2%	3,3%	1,9%
4240	2,8%	3,9%	3,2%	1,8%
4220	2,6%	3,7%	3,1%	1,8%
4200	2,4%	3,4%	2,9%	1,7%
4180	2,3%	3,2%	2,7%	1,6%
4160	2,1%	2,9%	2,5%	1,5%

Table 6.10: Option prices for the S&P 500 with the Heston Model (FDE) and its errors

6.5. Results for American put options

Having the quality of the Heston FDE Method proofed for European Call options, we are now switching the underlying dataset to do the same for American Put options. The Put option market values as well as the results using the CRR Method with an optimized volatility of 26.15% are shown in table 6.11. The

optimized volatility is retrieved from MatLab, where we manually lowered the mean absolute error between the actual and freshly calculated put option values for the 03.08.2021 to its minimum.

Market American Put Option Prices Apple 04.08.21				
	44	72	107	135
170	23,48	23,90	24,93	25,50
165	18,65	19,30	20,63	21,35
160	14,03	14,95	16,68	17,45
155	9,75	11,15	13,08	14,03
150	6,30	7,85	9,98	10,95
145	3,67	5,30	7,35	8,43
140	2,13	3,46	5,40	6,35
135	1,23	2,31	3,90	4,75

CRR American Put Option Prices Apple 04.08.21				
	44	72	107	135
170	23,37	23,96	24,79	25,47
165	18,72	19,55	20,60	21,39
160	14,35	15,44	16,69	17,59
155	10,40	11,73	13,13	14,11
150	7,03	8,50	9,98	11,00
145	4,36	5,82	7,29	8,30
140	2,44	3,73	5,08	6,03
135	1,20	2,22	3,36	4,19

Table 6.11: Option prices for the Apple stock from the market and with the CRR Method

The implied volatilities from table 6.1 are passed to the Heston FDE function in MatLab, resulting in the values and errors from table 6.12.

Heston FDE American Put Option Prices Apple 04.08.21				
	44	72	107	135
170	23,24	23,80	24,80	25,75
165	18,47	19,28	20,55	21,65
160	13,09	15,06	16,58	17,83
155	9,80	11,22	12,97	14,33
150	6,33	7,95	9,82	11,23
145	3,68	5,31	7,16	8,56
140	1,92	3,33	5,03	6,34
135	0,90	1,97	3,40	4,56

Heston FDE American Put Option Prices Apple 04.08.21 % Error				
	44	72	107	135
170	1,00%	0,42%	0,50%	0,98%
165	0,97%	0,10%	0,36%	1,41%
160	6,64%	0,74%	0,57%	2,18%
155	0,51%	0,63%	0,80%	2,17%
150	0,48%	1,27%	1,55%	2,56%
145	0,27%	0,19%	2,59%	1,54%
140	9,65%	3,76%	6,85%	0,16%
135	26,83%	14,53%	12,82%	4,00%

Table 6.12: Option prices for Apple with the Heston Model (FDE adaption) and its errors

From the heat map we can quickly see that the values are a good fit, except for OTM options. The values for close to ATM short term options are remarkably accurate. The RMAE for the FDE values is 3.41% comparing to 4.36% of the CRR ones. We can conclude that the Heston FDE performed better than the CRR Method for our data.

7. Discussion

After introducing the Heston Model and applying it to real market data, there are several conclusions to make, including advantages and disadvantages. The first and most important conclusion is that the Heston Model delivers closed form solutions for European options of good quality (table 6.5) and is able to outperform the peer model, the BSM. The numeric results with the Heston FDE for American options are more accurate than the peer model, the CRR, as well. Therefore, the model definitely has its value.

One reason for the good performance of the model is the fact, that it reflects real market data better than its peer model do. By using not a single value for the volatility, but five parameters, the Heston Model is able to reflect the characteristics of the underlying distribution (figures 5.1 and 5.2) and the behavior of the volatility as well (table 6.1). Furthermore, we were able to confirm the impact ρ and σ have on the results of the model, making our findings even more consistent.

A further advantage of the model is its great flexibility. The model can be adapted to different other methods, depending on how to solve the PDE in 4.24. This allows the model to calculate European and American options. Also, with different adaptions comes greater opportunities, making it more likely to find good results. For example, the best results we found for our European option data set were received using the FDE Method, even if it was not the actual idea to show so. The same flexibility goes for the objective function we minimize to calibrate the parameters. Since there are several results, we can see which one delivers the best one in the sense of IVMSE.

On the other hand, this flexibility adds some kind of uncertainty to the whole model. There are many choices to make, and there are no clear findings in the academia which one is the best for the final results. Specially the parameter calibration is very sensitive to changes in the objective function and the starting values. Examining this in more detail is beyond the scope of the thesis. Depending on the chosen loss function and possible adaptions to other models, we can see that the results may vary a lot. Therefore, results also are subject to some coincidence, leading in extreme cases to wrong conclusions.

One very important impact factor not discussed yet is the chosen market data. Obviously, the results are also depending on the size of the sample data, the maturity, the strike price range and the amount by which the underlying price changes in one day. We can see this already from the change from table 6.5 to table 6.8. Again, a further examination of the relationships is of this thesis' scope. Nevertheless, it is important to be aware of them when putting the results in perspective.

During the calculations with the BSM Model, we discovered results worth mentioning here as well. When we do not use an optimized, single volatility for the BSM results, but use the individual implied volatility of every option to calculate its values the next day, we outperform all shown results. E.g., using a volatility

of 17.68% for the European option with a strike price of 4200 and a maturity of 73 days (from table 6.1) and so forth, we only receive an RMAE of 1.93%. Obviously, this result is not directly comparable to the Heston Model values we found, since it uses not a single volatility as a parameter, but 116. Nevertheless, receiving these results does not require the mathematical level of the Heston Model, is very easy and intuitive and delivers better results, which can be found in table 7.1. Results like this might question the effort needed to receive values with the Heston Model.

Individual IV Black Scholes Option Prices 04.08.21				
	44	72	107	135
4720	1,28	7,22	19,23	31,24
4700	1,71	8,83	22,47	35,63
4680	2,30	10,75	26,23	40,50
4660	2,87	13,15	30,56	45,96
4640	3,90	16,06	35,47	51,90
4620	5,29	19,60	41,00	58,48
4600	7,14	23,80	47,21	65,60
4580	9,75	28,75	54,06	73,32
4560	12,94	34,61	61,60	81,64
4540	17,25	41,25	69,79	90,50
4520	22,59	48,82	78,68	99,98
4500	29,27	57,39	88,23	109,91
4480	36,90	66,58	98,34	120,35
4460	45,88	76,82	109,16	131,30
4440	56,09	87,80	120,40	142,71
4420	67,31	99,50	132,31	154,54
4400	79,43	111,88	144,68	166,88
4380	92,53	124,85	157,48	179,58
4360	106,29	138,35	170,64	192,60
4340	120,67	152,28	184,23	205,93
4320	135,61	166,65	198,18	219,58
4300	150,90	181,45	212,45	233,54
4280	166,85	196,63	227,04	247,81
4260	182,94	212,03	241,80	262,35
4240	199,37	227,71	256,88	276,90
4220	216,03	243,66	272,27	291,91
4200	232,88	259,84	287,87	307,14
4180	250,06	276,23	303,70	322,48
4160	267,37	292,75	319,63	338,12

Table 7.1: BSM option prices for the S&P500 using individual implied volatilities

8. Conclusion

The objective of this work was to introduce the Heston Model theoretically and test it practically in a numerical study. To do so, we started with essential basics of option valuation and stochastic process. Guided by Heston (1993) and Rouah (2013), the derivation of the model was presented in detail to completely understand it. Afterwards, the model was examined and extended with optimizations, specially done by Albrecher et al (2007), but others as well. The problems were shown in 3D-surfaces, making them easier to grasp. To use the model for American options, we also introduced the FDE Method, which is applicable in the Heston Model as well. Having all theoretics introduced, we conducted a sensitivity analysis, giving insights into the relationships between the parameters and the calculated model option values. We showed that the Heston Model is able to reflect the characteristics of financial data-distributions better than a standard normal distribution, which is used in the BSM Model.

In the main part of this work, the application of the Heston Model using real market data, we found positive results as well. During the sensitive calibration process we introduced different objective function, which delivered different values for the parameters. For our data sample we proofed that calibrated parameters indeed reflect the distribution in a more realistic way with the results being in line with the previous parameter analysis. Regarding the model performance, the standard Heston Model was able to outperform the peer model, the BSM Model. Same was the case for the application of the FDE in the Heston Model, which outperformed the CRR. The overall errors found lie within an acceptable range, making the results valid not only relative, but also absolute. Next to the overall results, we were also able to confirm the behavior of the option price within one sample and compered to the results of the BSM Model. On the other hand, the idea of using split sample data to optimize the overall RMAE of the standard Heston Model failed, since the results worsened. In the discussion we summed up the advantages and disadvantages of the Heston Model that we find during our work.

Over the course of the thesis, we showed many results, but discovered even more open points to further act on. Using different underlying datasets, longer maturities, wider data ranges, other Heston Model applications, etc. are strongly interesting. The goal would be to keep on improving the valuation of derivatives and option in particular, continue were Heston started with his idea.

Bibliographical References

Abken, P. A. & Nandi, S., 1996. Options and Volatility. *Economic Review, 81(3-6).*

Albrecher, H., Mayer, P., Schoutens, W. & Tistaert, J., 2007. The little Heston trap. *Wilmott, (1).*

Attari, M., 2004. Option pricing using Fourier transforms: A numerically efficient simplification.

Black, F. & Scholes, M., 1973. The Pricing of Options and Corporate Liabilities. *The Journal of Political Economy, Vol. 81, No. 3*.

Brennan, Michael J. und Schwartz, Eduardo S. (1978): Finite Difference Methods and Jump Processes Arising in the Pricing of Contingent Claims: A Synthesis. *The Journal of Financial and Quantitative Analysis*, *Vol. 13 No. 3.*

Cox, J. C.,1996. The Constant Elasticity of Variance Option Pricing Models. *Journal of Portfolio Management.*

Cox, J. C., Ingersoll Jr, J. E. & Ross, S. A., 1985. An intertemporal general equilibrium model of asset prices. *Econometrica: Journal of the Econometric Society*.

Cox, J. C., Ross, S. A. & Rubinstein, M., 1979. Option Pricing: A Simplified Approach. *Journal of Financial Economics 7*.

Darling, D. A. & Siegert, A. J. F., 1953. The first passage problem for a continuous Markov process. *The Annals of Mathematical Statistics*.

Dixit, R. & Pindyck, R., 1994. Chapter 3. Stochastic Processes and Ito's Lemma. *Investment under Uncertainty*.

Guillaume, F., and W. Schoutens. (2012). ‘‘Use a Reduced Heston or Reduce the Use of Heston?’’ *Wilmott Journal, 2 (4).*

Heston, S. L., 1993. A Closed-Form Solution for Options with Stochastic Volatility with Applications to Bond and Currency. *The Review of Financial Studies Vol. 6, Nr. 2*.

Hull, J. C., 2018. *Options, futures, and other derivatives.* 10 ed. s.l.:Pearson.

Itô, K., 1951. *On stochastic differential equations (No. 4).* s.l.:American Mathematical Soc.

Jacquier, E. & Jarrow, R., 2000. Bayesian analysis of contingent claim model error. *Journal of Econometrics, 94 (1-2)*.

Kahl, C. & Jäckel, P., 2005. Not-so-complex logarithms in the Heston model. *Wilmott magazine, 19 (9)*.

Lewis, A. L., 2000. The Fundamental Tranform. In: *Option Valuation under Stochastic Volatility.* Newport Beach, CA: Finance Press.

Longstaff, F. A. & Schwartz, E. S., 2001. Valuing American Options by Simulation: A Simple Least-Squares Approach. *The Review of Financial Studies Spring Vol. 14, No. 1*.

Merton, R. C., 1973. Theory of rational option pricing. *The Bell Journal of economics and management science*.

Mikhailov, S. & Nögel, U., 2004. Heston's stochastic volatility model: Implementation, calibration and some extensions. In: *The Best of Wilmott 1 Incorporating the Quantitative Finance Review.* s.l.:John Wiley and Sons.

Mondal, M., Alim, M., Rahman, M. & Biswas, M., 2017. Mathematical Analysis of Financial Model on Market Price with Stochastic Volatility. *Journal of Mathematical Finance, 7*.

Nagel, H., 2001. *Optionsbewertung bei stochastischer Volatilität.* s.l.:Springer Fachmedien Wiesbaden.

Paul, W. & Baschnagel, J., 2013. *Stochastic Processes From Physics to Finance 2nd Edition.* s.l.:Springer.

Rouah, F. D., 2013. *The Heston Model and Its Extensions in Matlab and C#.* s.l.:Wiley.

Samuelson, P. A., 1973. Mathematics of speculative price. *Siam Review, 15 (1)*.

Zhu, J., 2010. *Applications of Fourier transform to smile modeling: Theory and implementation.* 2nd Edition ed. s.l.:Springer Science & Business Media.